BIOMECHANICAL CHARACTERIZATION OF EXTENSOR DIGITORUM LONGUS, FLEXOR DIGITORUM LONGUS, FLEXOR HALLUCIS LONGUS, AND PERONEUS BREVIS TENDONS AS VIABLE ACL REPLACEMENTS
AND
MARATHON SIMULATION TO DETERMINE PHYSIOLOGICAL RESPONSES TO CYCLIC LOADING

By

MERIDITH R MYRICK

A THESIS PRESENTED TO THE GRADUATE SCHOOL
OF THE UNIVERSITY OF FLORIDA IN PARTIAL FULFILLMENT
OF THE REQUIREMENTS FOR THE DEGREE OF
MASTER OF SCIENCE

UNIVERSITY OF FLORIDA

2009

To Pedro D. Pedroso, who pursues excellence with a passion and encourages others to join in this endeavor

ACKNOWLEDGMENTS

I thank RTI Biologics, Inc. for providing the time, resources, and guidance necessary to complete my thesis. I have been blessed to work with a brilliant and caring team of people who have helped me to grow in so many ways. I give a special thanks and acknowledgement to Pedro Pedroso for encouraging me to pursue my thesis and for always providing guidance and expertise. I am grateful to Arunas Zhukauskas for sharing his four little tendons with me and for sharing his wisdom and experience.

I could not have completed my thesis without the cooperation and guidance of my committee chair, Dr. Scott Banks, and my committee members, Dr. Malisa Sarntinoranont and Dr. Benjamin Fregly, and to them I am grateful.

I would also like to thank my patient and wonderful fiancé, who knows more about tendons than any electrical engineer should. He is my champion. God has blessed me with a family who loves me and supports me through all of my endeavors, and with this security comes the confidence to pursue new challenges. Lastly, or rather firstly, I would like to thank Ms. Rebecca Austin for the spark. I have been fortified beyond measure.

TABLE OF CONTENTS

LIST OF TABLES

LIST OF FIGURES

LIST OF ABBREVIATIONS

CDC	Centers for Disease Control and Prevention
ACL	Anterior cruciate ligament
EDL	Extensor digitorum longus
FDL	Flexor digitorum longus
FHL	Flexor hallucis longus
PB	Peroneus brevis
AT	Anterior tibialis
UTF	Ultimate tensile force
UTS	Ultimate tensile stress
UTε	Ultimate tensile strain
UText	Ultimate tensile extension
E	Young’s modulus
CSA	Cross-sectional area

Abstract of Thesis Presented to the Graduate School
of the University of Florida in Partial Fulfillment of the
Requirements for the Master of Science

BIOMECHANICAL CHARACTERIZATION OF EXTENSOR DIGITORUM LONGUS, FLEXOR DIGITORUM LONGUS, FLEXOR HALLUCIS LONGUS, AND PERONEUS BREVIS TENDONS AS VIABLE ACL REPLACEMENTS
AND
MARATHON SIMULATION TO DETERMINE PHYSIOLOGICAL RESPONSES TO CYCLIC LOADING

By

Meridith Myrick

December 2009

Chair: Scott Banks
Major: Biomedical Engineering

The incidence of anterior cruciate ligament (ACL) replacement surgeries in the US is estimated to reach nearly 350,000 per year. Utilization of allograft tissue as a regenerative approach to tissue engineering can aid in restoration of native ACL biomechanics, while also preventing donor site defects associated with autologous grafts. A limited supply of allograft tissue motivates further investigation of alternative graft sources; therefore, biomechanical characterization of extensor digitorum longus (EDL), flexor digitorum longus (FDL), flexor hallucis longus (FHL), and peroneus brevis (PB) was performed in order to determine their efficacy as potential ACL replacements in a double strand configuration. Values achieved in testing anterior tibialis (AT) were used as a comparison because of its acceptance and current use as an ACL allograft. Tensile testing with a load-to-failure protocol was performed on all five tendons. Average ultimate tensile force (UTF) values for single strands of EDL, FDL, FHL, and PB were 1136.5 ± 291.8 N (n=36), 954.1 ± 270.5 N (n=36), 1156.3 ± 348.0 N (n=36), and 1285.9 ± 300.0 N (n=44). Single strand AT had an average UTF of 2122.3 ± 574.7

N (n= 412) and an average ultimate tensile stress (UTS) of 91.05 ± 28.04 MPa. Average UTS values were 134.59 ± 36.0 MPa, 99.45 ± 25.9 MPa, 101.98 ± 28.9 MPa, and 87.85 ± 22.5 MPa for EDL, FDL, FHL, and PB. With this data, it was shown that EDL has a statistically greater Young's modulus of elasticity value and greater UTS value than AT ($p>0.05$). It was concluded that EDL, FDL, FHL, and PB provide viable sources as allograft tissue for ACL replacement if implemented as double strand grafts.

To further characterize allograft tendons, AT was used to perform physiologic cyclic loading like that experienced by the native ACL during a simulated marathon. The average Young's modulus of elasticity over 11,712 cycles was 382.0 ± 133.16 MPa and damage accumulation was observed in 7 of the 20 specimens. Average dynamic creep of twenty samples was 0.078 ± 0.039 mm/mm, and a trend of increased strain was associated with decreased Young's modulus values. Negative hysteresis trends indicated decreased cyclic energy dissipation; however, no correlation was found between damage accumulation and hysteresis value. All tendons performed without failure, and a validation test confirmed that even with evidence of damage accumulation, the tendon was able to maintain its tensile strength.

CHAPTER 1
INTRODUCTION

Anterior Cruciate Ligament Replacement

The use of allograft tissue for reparative surgeries is an increasing trend, but resources are limited to the number of available donors. Anterior cruciate ligament (ACL) reconstructions are estimated to reach nearly 350,000 in the United States each year, and this trend is growing by about 5% yearly[1,2]. Nearly 2.3 million orthopaedic soft tissue procedures were performed in the US in 2008[2], and the CDC estimated that 1.5 million bone and tissue allografts are distributed yearly by American Association of Tissue Banks-accredited tissue banks in the United States[3,4]. With a growing demand for tissues reaching 1.5 million[3], and a limited number of donors, an investigation into alternative viable tissues for ACL replacement was conducted. Characterization included the following tendons: extensor digitorum longus (EDL), flexor digitorum longus (FDL), flexor hallucis longus (FHL), peroneus brevis, and anterior tibialis (AT) tendon. Alternative sources of allograft material better utilize the gift of donor tissue, and provide an efficient and economically attractive source of additional graft material.

To the author's knowledge, no previous biomechanical evaluation has been performed on the FHL, EDL, PB, or FDL as viable ACL replacements. These grafts were tested to determine if, when doubled, they would perform comparable to the native ACL. According to different implant techniques, double or even quadruple strands could be applied as allografts. The AT tendon also was tested to serve as a comparison graft because of its popularity as allograft tissue and the available mechanical property values reported in literature. To further characterize allograft tendons, AT was used to

perform physiologic cyclic loading like that experienced by the native ACL during a simulated marathon.

Sports-related injuries are the most common sources of knee injuries, and these injuries most often manifest in tears of the ACL, which greatly reduces the stability of the knee joint[2]. In 2008, 334,500 ACL reconstructions were performed, and it is predicted that 423,700 reconstructions will be performed annually by the year 2013[2]. The total cost of knee ligament reconstruction grafts and devices in 2008 totaled about $435 million, and this area of orthopaedics will only continue to grow as an ageing population continues to pursue active lifestyles and incur more sports-related injuries[2,5]. In addition, women are more likely to sustain ACL injuries than men, and their increased participation in sports will further increase the need for knee ligament reconstructions[5].

Ligament damage in the knee can occur when a sudden motion, hyperextension, or flexion causes damage to the ligament[2]. Sports requiring cutting motions are most associated with this type of ligament damage and include football, basketball, and volleyball[2,5]. In addition to the abrupt rupture or tear of the ACL due to this motion, it has been established that tendons could sustain damage due to the failure of a cyclically loaded tissue under higher stresses or through time-dependent mechanisms in cycling, or by a combination of the two[6.] This type of motion could be observed during a run in which repetitive loading is experienced by the ACL. To address both mechanisms of tendon damage, in vitro tendon testing was performed to determine tendon response under both ultimate tensile loads in a load-to-failure test protocol and under repetitive cyclic loading which simulated marathon forces and frequency.

Graft Utilization

Since the first ACL reconstruction in 1917, many new grafts and many new techniques have been implemented[7]. The use of allografts is a growing trend for multiple reasons and graft selection and fixation technique can be specialized based on patient needs and activity level. To this end, surgeons may select tendons with bone blocks or pure soft tissue (with the necessary fixation hardware) and they may choose the double strand technique or the single strand technique. To achieve the double strand orientation, some surgeons will "loop" the tendon, folding it in half and subsequently making two strands out of one tendon. In other cases, a double strand configuration is achieved by applying two single strand tendons as one graft.

While there are merits to both autografts and allografts, the advantages of using allograft tissue include: no donor site morbidity, reduced operating time for surgeons, unaltered patellofemoral tracking and thigh muscle function, unlimited available sizes, and smaller surgical incisions[4,8,9]. Additionally, allograft tissue may be a necessary selection for revision ACL surgery if the patient formerly received an autologous graft.

Allograft Tendons

Multiple graft sources are utilized for allograft reconstruction, the two most common tendon grafts being the patellar tendon and a combination of gracilis and semitendinosus tendons[10,11]. Other common graft sources for ACL replacement include achilles tendon, quadriceps tendon, anterior tibialis, and posterior tibialis[1,4,9,12]. Depending on the size and the location of the harvested tendon, the graft may be implanted as a single strand or as a double strand. The number of strands applied depends on surgeon preference and/or whether bone blocks are present with the graft tissue.

The double strand technique is suggested to more closely resemble the mechanics of the native ACL, and thus provide greater stability. However, depending on the technique of implantation utilized, four tunnels may be necessary instead of the standard two[7,13]. The rate of graft healing within bone tunnels is a result of the size and number of the tunnels that must be produced for proper graft fixation[13]. Grafts composed of all soft tissue, therefore containing no bone blocks, have been shown to sustain loads adequate for native ACL activity, while also minimizing the necessary bone tunnel size for fixation[9].

While the merits of allograft tendons are numerous with regards to reconstructive purposes, a concern lies with the issue of sterility. To mitigate this concern, tissues can be sterilized to remove or inactivate organisms. The primary methods of sterilization for tendon tissue are through gamma irradiation, cryoprotectant incubation, and/or through proprietary chemical processing[4]. According to the FDA, achievement of sterility is attained for biological medical devices at an assurance level of 10^{-3} (1 in 1000 chance of a living microbe existing in the tissue) [4]. Greater regulations have been implemented since May 2005 regarding "Current Good Tissue Practices" in an effort to prevent disease transmission through reconstructive surgeries[3].

Characteristics of the ACL and its Replacement Grafts

In vitro testing of tendons, like the tests performed in the author's present study, have been performed in order to determine the efficacy of different tendons as replacements for the ACL[10,14,15]. Challenges exist in testing tendons, and the mitigating solutions to these challenges can affect final mechanical results. Factors to take into consideration include hydration, temperature, gripping method, preconditioning, and tendon type and number (i.e. single, double, looped). A literature review is provided in

which the biomechanics of different tendons are described. Ultimate tensile force (UTF) and ultimate tensile stress (UTS) graft comparisons are displayed in Figure 1-1 and Figure 1-2, respectively.

ACL. The ACL is consists of the anteromedial bundle (AM) and the posterolateral bundle (PM), which extends from the lateral femoral condyle within the intercondylar notch to an insertion at the anterior part of the central tibial plateau[7]. The length of the ACL ranges from about 22 mm to about 41 mm and its width averages about 7 mm to 12 mm[13]. The cross-sectional area is not uniform and increases from the femur to the tibia[13,16]. In a pull-to-failure test, Noyes et al. reported a UTF of the native ACL of younger donors as 1725 ± 269 N with a maximum stress of 37.8 ±3.8 MPa [14,17,18]. While the ACL is recorded to fail at loads exceeding about 1725 N, it is estimated that the native ACL experiences only approximately 250 N during ambulation, and only approximately 454 N for most activities[14,17,18].

Obvious variations in the results for Young's modulus of elasticity values amongst different tendons, as well as tendons of the same type, indicate that determining this parameter is sensitive to many factors[10,14,15,19,20]. Young's modulus is a material property; therefore, its values are expected to be relatively constant, or at least consistent. Tendons and ligaments, however, are viscoelastic in nature, and environmental factors such as temperature and hydration directly affect this property[21,22]. Noyes et al. calculated the Young's modulus of the ACL for adults aged 48-86 years old at a value of 65.3 ± 24 MPa and a value of 111 ± 26 MPa for the human ACL of donors aged 16- 26 years old[17]. Butler et al. later tested the AM and PL bundles

of the ACL separately and found Young's modulus values of 283 ± 114 MPa and 154 ± 120 MPa, respectively[23,24]

Bone-patellar-tendon-bone. The central portion of the bone-patellar-tendon-bone (BPTB) graft displayed a UTF of 2900 ± 260 N, which is about 168% the UTF of the native ACL[18]. With an average area of 50.5 ± 2.8 mm², this results in a UTS of 58.3 ± 6.1 MPa[18]. Of the grafts listed for comparison, BPTB provides the greatest UTF value as a single one-stranded alternative to the ACL, and its cross-sectional area indicates the reason that it is applied as a single stranded graft.

Hamstring and semitendinosus tendons. The hamstring tendons, semitendinosus and gracilis, are tested as single strands or as double strands, with either a combination of the two tendons, or two of the same tendons. When the double stranded tendons are tested, an important factor in determining the combined tensile properties is that tension is applied equally to both tendons[10]. Biomechanical observation of the double-strand approach displays the additive effect of applying multiple strands, and this physical law is observed through previous work[10,15]. One stranded semitendinosus tendon with an average area of 10.8 ± 2.2 mm² has a UTF of 1060 ± 227N and a UTS of 99.3 ± 14.9 MPa[10]. One stranded gracilis tendon with an average area of 7.4± 1.1 mm² has a lower UTF of 837 ± 138 N and a higher UTS of 113.1 ± 18.1 MPa[10].

Anterior and posterior tibialis tendons. Anterior and posterior tibialis tendons perform similarly, with no significant difference in the values reported for UTF (p= 0.53)[15,20]. Pearsall et al. reported a UTF of 3412 N for the two-stranded AT tendon[20], and Taut et al. reported a UTF of 4122 ± 893 N for the looped double strand AT

tendon[15]. Additionally, Pearsall et al. reported a UTF value of 3391 N for the two-stranded posterior tibialis tendons[15], and Taut et al. reported a UTF value 3594 ± 1330 N for the looped double strand posterior tibialis tendon[20]. UTS values range from about 85 MPa to 108 MPa for both tendon types by each investigator of the double strand methods[15,20]. When doubled, the area of these tendons is comparable to that of the native ACL (p= 0.35), and their UTF values are about 200% that of the native ACL [15,18,20].

Young's modulus values for AT varied in magnitude according to different studies. Haut et al. recorded a value of 847 ± 301 MPa for the looped double strand method[15], yet Pearsall, et al. reported Young's modulus results as low as 0.243 MPa[20]. An interesting in vivo study was performed by Maganaris et al. in which the Young's modulus was determined at different forces[25]. At an in vivo force of 71 ± 12 N, a Young's modulus was recorded as 450 ± 60 MPa, and at an in vivo force of 530 ± 59 N, Young's modulus values were recorded at 1200 ± 150 MPa[25]. The difference in Young's modulus at these different forces could be a result of straightening of the fiber crimp as the applied force increased.

EDL, FDL, FHL, PB, and AT Anatomy

The tendons EDL, FDL, FHL, and PB contribute to the muscles of the ankle and foot. These muscle/tendon complexes steady the tibia and fibula perpendicularly on the talus, thus helping to maintain an upright posture and helping to give strength to the ankle-joint. Figure 1-3 displays these tendons.

The EDL tendon lies on the lateral portion of the front of the leg, and the AT tendon lies on its medial side and the peronaei lie on its lateral side. The EDL divides into four strands and runs forward on the dorsum of the foot to the four lesser toes.

With this conformation, EDL acts to extend the phalanges of the toes and flex the foot upon the leg. Measurement of the EDL tendon from a donor leg-en-bloc of the tibia/fibula portion was about 250 mm.

The FDL tendon is located on the tibial side of the leg, and the muscle that it supports curls the second, third, fourth and fifth toes. As it passes into the sole of the foot, it crosses below the FHL tendon and is joined in a tendinous slip. It then divides into four tendons which are inserted into the phalanges of the lesser toes. In this way, it is the antagonist muscle/tendon complex of the EDL. Measurement of the FDL tendon from a donor leg en bloc of the tibia/fibula portion was about 230 mm.

The FHL tendon is located on the posterior compartment of the fibular side of the leg and occupies nearly the whole length of the posterior surface of the muscle. It runs along the sole of the foot and is inserted into the last phalanx of the great toe where it is situated above and crosses from lateral to medial side of the FDL tendon, where it is connected by a fibrous slip. FDL and FHL are direct flexors of the phalanges, and extend the foot upon the leg to assist the Gastrocnemius and Soleus in extending the foot. This allows the actions of walking or standing on tiptoe. Measurement of the FHL tendon from a donor leg en bloc of the tibia/fibula portion was about 180 mm.

The PB muscle lies under the peroneus longus muscle, and its tendon is shorter and smaller than the other tendons, EDL, FDL, and FHL. The fibers of the muscle pass downward and end in the PB tendon, which runs behind the lateral malleolus. The peroneus longus and PB tendons proceed within the same compartment via a common mucous sheath. PB tendon then passes down the outside of the lower leg and everts the foot, attaching the fifth metatarsal to the outside of the foot. The peroneus longus

and PB thus extend the foot upon the leg, acting against the AT and peroneus tertius, which are flexors of the foot. Measurement of the PB tendon from a donor leg en bloc of the tibia/fibula portion was about 180 mm.

Finally, the AT tendon located on the lateral side of the tibia and is inserted into the base of the first metatarsal bone. It is attached to the most medial muscle of the anterior compartment of the leg and is a direct flexor of the foot at the ankle joint, acting with peroneus tertius. When acting in conjunction with posterior tibialis, it raises the medial border of the foot, inverting it and stabilizing the ankle as the foot hits the ground in walking.

The five tendons were tested for their average Young's modulus value, average UTF, average UTS, average ultimate tensile strain (UTε), and average ultimate tensile extension (UText). The aim of this analysis was to determine the potential use of the EDL, FDL, FHL, and PB as viable ACL replacement tendons, therefore, maximizing utilization of donor tissue. To further predict allograft performance, a marathon simulation utilizing AT was performed and the properties dynamic creep, strain, extension, hysteresis, and Young's modulus were calculated over 11,712 cycles to display tendon response to long-term cyclic loading.

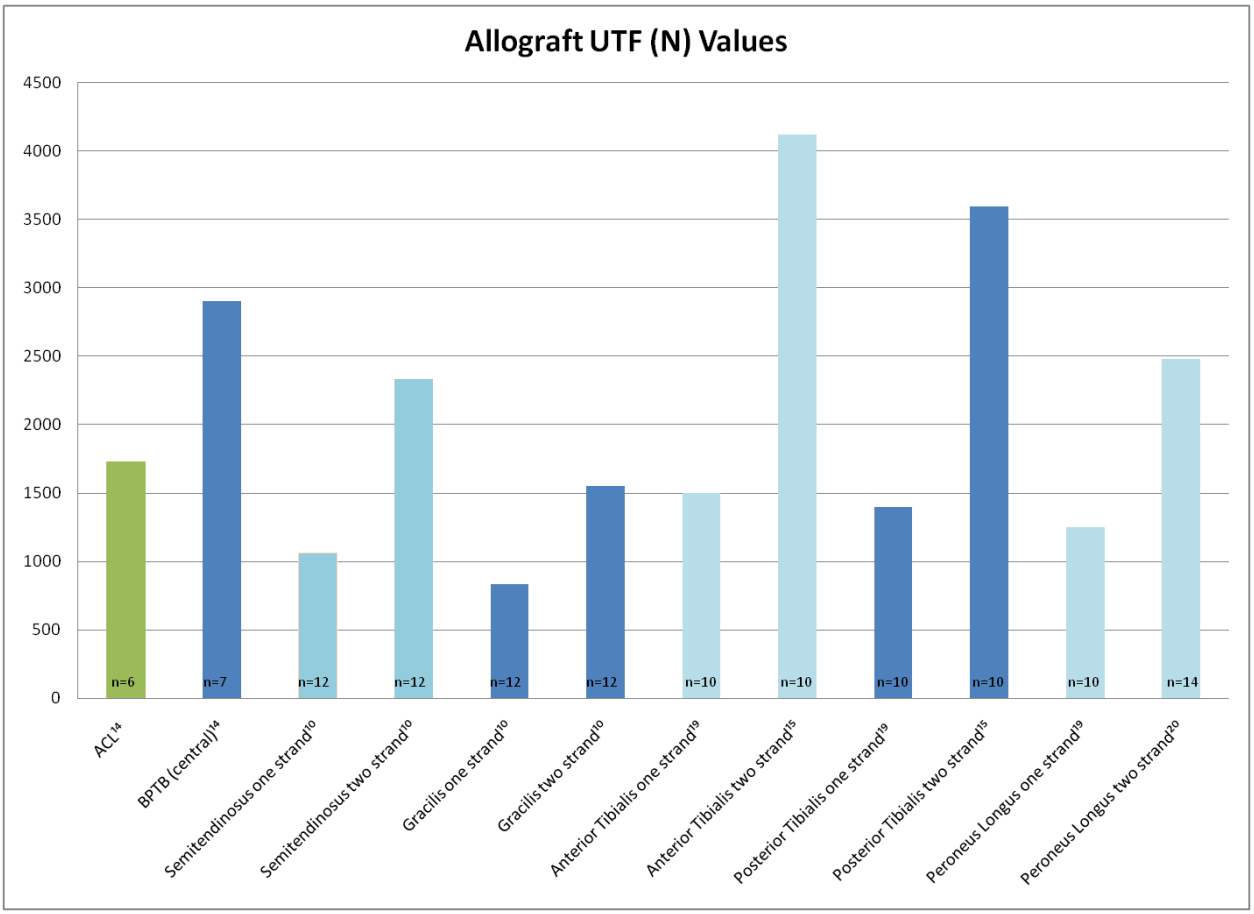

Figure 1-1. Average UTF values of accepted allograft tendons for ACL replacement.

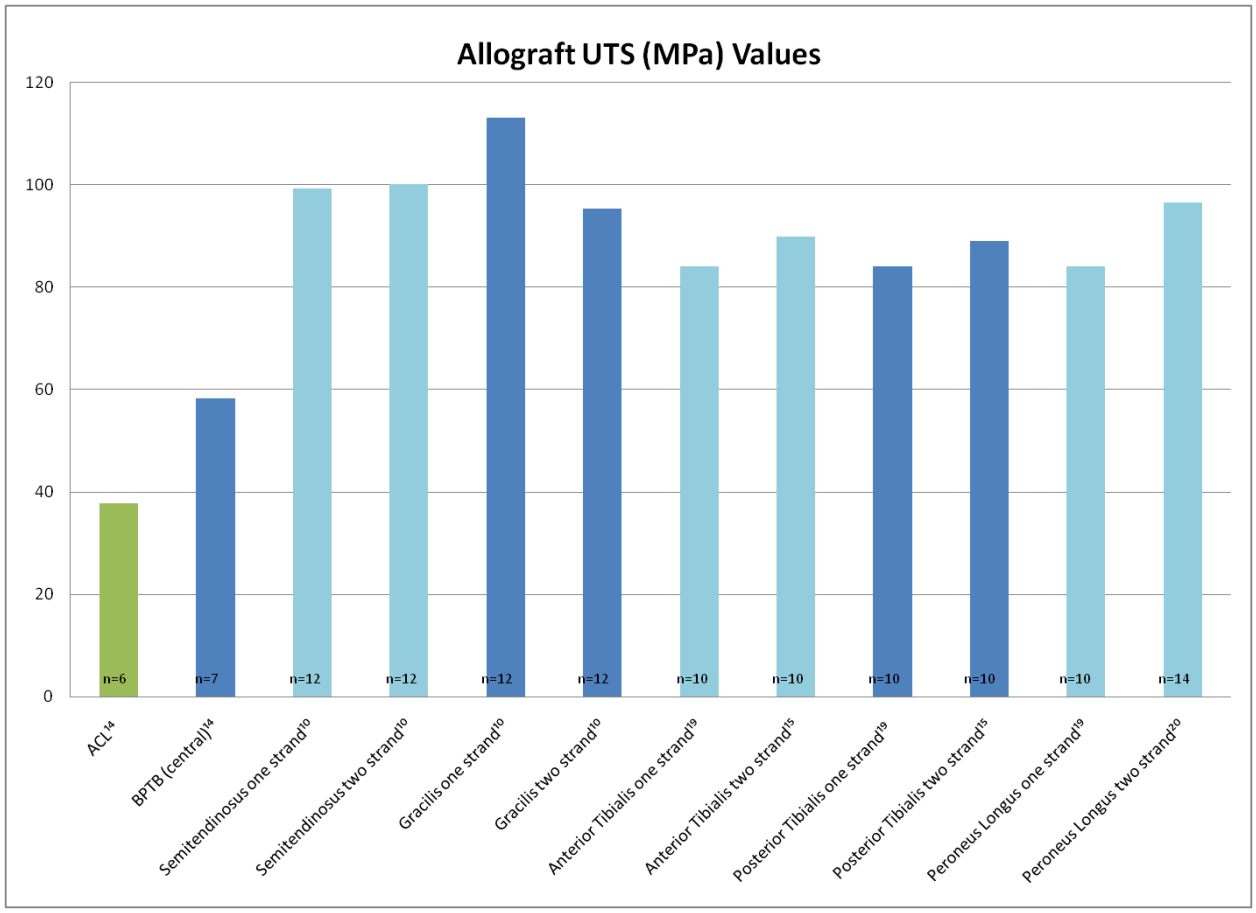

Figure 1-2. Average UTS values of accepted allograft tendons for ACL replacement

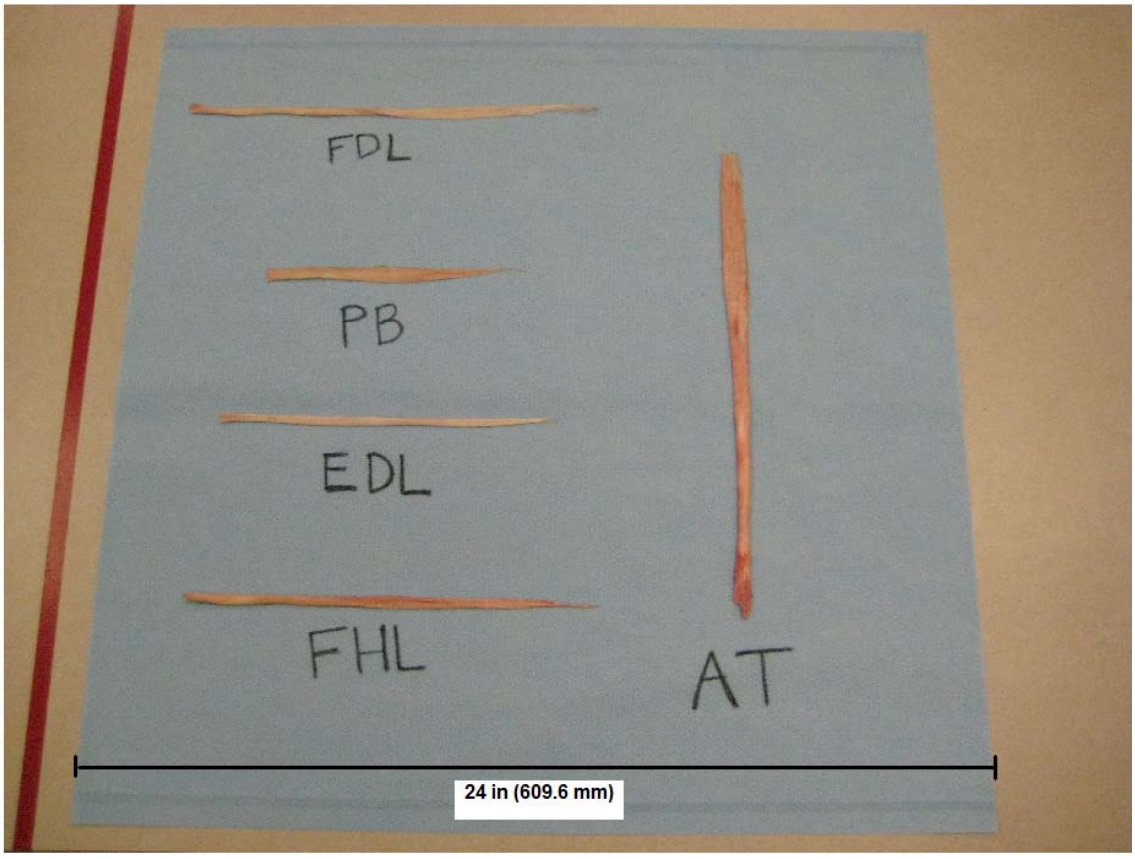

Figure 1-3. FDL, PB, EDL, FHL, and AT tendon comparison.

CHAPTER 2
MATERIALS AND METHODS I

Tissue Allocation

All donor tissue was obtained through RTI Biologics, Inc. A minimum of 36 samples accounted for each tendon type. A possibility of two samples were retrieved from one tendon, one distal and one proximal in orientation. Therefore, four samples could originate from a single donor in the event that tendons were recovered from both legs of a donor. All tendons were recovered according to criteria established by the FDA and the American Association of Tissue Banks. The tendons were stored in -70º C until the day of testing, and at the time of testing, they were thawed in 0.9% saline at room temperature for a minimum of thirty minutes.

Load-to-Failure Test

Tendon Preparation

Thirty-six EDL samples were acquired, constituting ten donors aged 32 years to 76 years with an average age of 54.1 years old. Thirty-six FDL samples were acquired, constituting eleven donors aged 29 years to 82 years with an average age of 63.64 years old. Thirty-six FHL samples were acquired, constituting eleven donors aged 29 years to 82 years with an average age of 57.9 years old. Forty-four PB samples were acquired, constituting fourteen donors aged 22 years to 70 years with an average age of 49.1 years old. EDL, FDL, FHL, and PB tendons were all aseptically processed.

Four-hundred twelve AT samples were acquired, aged 15 to 94 years old with an average of 57.5 years. One hundred thirteen donors contributed to this sample size, and these tendons were all sterilized through the BioCleanse© sterilization process. AT tendons contributing to the author's comparison study were also applied to other

research aims, which explains the selection for a large sample size and the reasoning for sterilized tendons. Additionally, the fact that the AT tendons were sterilized did not alter the biomechanical results achieved. Schmizzi et al performed a study comparing tendons processed through the BioCleanse© sterilization process to those aseptically processed and no significant differences were found between the two groups after the first cycle was performed and no significant differences were found in tendon failure loads[26].

A length of approximately 35 mm was measured in the center of each sample with about 20 mm remaining on each end for gripping. The gage length of 35 mm was distinguished to closely match the length of the ACL between tibia and femur insertions, which typically ranges between 22 mm to 41 mm[13]. Measurements were recorded using Mitutoyo IP67 digital calipers. Major and minor dimensions were measured in three locations along the sample and averaged to calculate an average cross-sectional area[27]. Major and minor dimensions were calculated for gage repeatability and reproducibility, and acceptable levels were found at 6.14% and 11.93% contribution in measurement variation.

Gripping Mechanism

Gripping of the tendons was achieved using custom-designed CryoGrips provided by RTI Biologics, Inc. Studies of the factors associated with this gripping method have been reported, and many researchers have adopted similar gripping methods[10,15,20]. No slippage of the tendon occurred with the application of the CryoGrip. Both ends of the tendon were clamped between grooved surfaces such that the tendon “snakes” around the grooves for a better hold. Dry ice was packed in a cooler that fit around each grip in order to freeze the tendon end to the gripper as one system. A warm-water jacket was

folded over the exposed tendon, and water was circulated within the tubing of this jacket such that the tendon was maintained at a temperature of about 37ºC (body temperature). This configuration allowed the ends of the tendon to be frozen to the grips while maintaining a temperature of about 37ºC along the mid-substance of the tendon that was to be tested. The necessary freeze timing depended upon on the thickness of the tendon. The AT tendons were allowed fifteen minutes to completely freeze to the grips, and the EDL, FDL, FHL, and PB were allowed eleven minutes for freezing. Figure 2-1 illustrates the CryoGrip configuration.

Test Method

Testing was performed using an MTS 858 Bionix testing system, and Multiworks software was utilized to record the time, extension, and force applied to the sample throughout the test. The tensile test included three operations, which involved three 90N holds for one minute each, one hundred cycles at loads of 50N to 250N, and a load-to-failure of the tendon at 50 mm/min. Figure 2-2 summarizes this testing sequence.

The 90 N hold serves as a preconditioning element for the tendon, simulating what many surgeons practice before implanting a tendon for reconstructive surgery[7]. This 90 N hold helps to straighten out the crimp in the collagen fibers associated with the toe-region of the stress-strain curve[28,29]. Thus straightening the crimp results in a linear stress-strain curve[28,29]. The load profile during cycling replicates the forces experienced by the ACL during normal ambulation[18]. Finally, the load-to-failure provides ultimate tensile properties of the tendon in the case of maximum utility of the tendon. Failure mode was recorded, with mid-substance failures being the ideal, and most frequent,

mode of failure. The properties that were derived from this test included UTF, UTS, UTε, UText, and Young's modulus.

Statistical Methods

Power and Sample Size

Sample size was calculated using MiniTab Statistical software. A power of 0.9 was selected for all sample size calculations. Sample sizes were determined using one-way ANOVA calculations with five levels for the EDL, FDL, FHL, PB, and AT tendons. All standard deviation values were obtained from a dataset of 245 AT tendons that had already been tested by the author. Practical differences were deduced from findings in literature. Noyes et al. stated that the ACL will experience a maximum of about 450 N during normal activity[18]. Blythe et al., however, suggested that a value of 700 N allows a greater factor of safety; therefore this value was applied in the author's study in the event that athletic events, etc. should require forces exceeding 450 N[11]. The UTS practical difference was calculated from the adopted 700 N practical difference and divided by the average cross-sectional area of the 245 AT tendons. The practical difference recorded for strain was based on an in vivo determination by Duthon et al. in which he found the natural elongation of the native ACL in different flexion orientations[30]. Based on the stress and strain parameters, Young's modulus was calculated. With these constants, sample sizes for each parameter were calculated and the largest sample size was applied. This ensured adequate resolution for calculations and comparisons. Table 2-1 displays the practical differences and standard deviations utilized for calculating sample size.

Comparative Analysis

Comparisons of variation between the five tendon cohorts utilized Bartlett's test. For results displaying equal variances ($p \geq 0.05$), one-way ANOVA was applied to determine if any significant differences were detected. If so, Tukey's 95% confidence interval of pair-wise comparisons was conducted to determine the tendon cohorts that were statistically different. If Bartlett's test indicated unequal variance, a Browne-Forsythe f-test was executed. If significant differences were detected, Welch's t-test was utilized to determine the tendon cohorts that were statistically different.

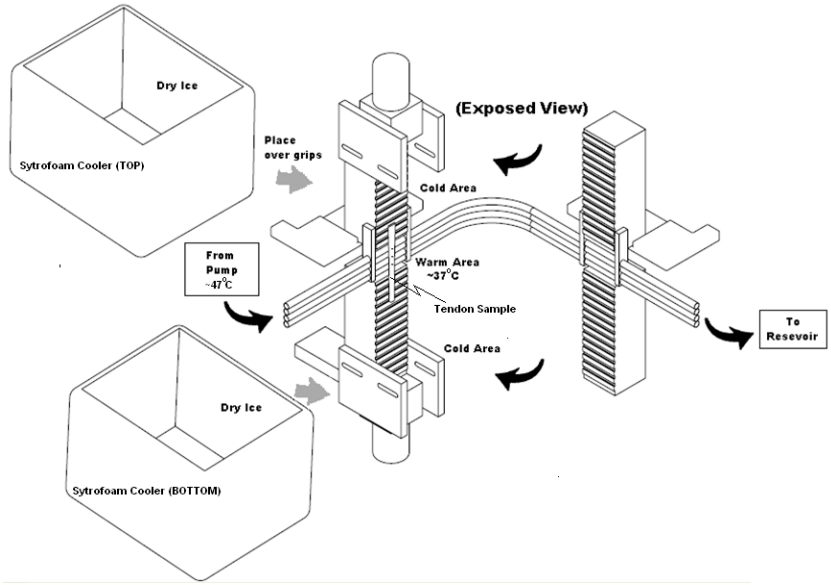

Figure 2-1. CryoGrip design. Coolers contain dry ice which freezes the ends of the tendon to the grip. A warm-water jacket surrounds the tested tendon portion in order to maintain a tissue temperature near 37ºC for testing. Permission for image use provided by Pedro Pedroso.

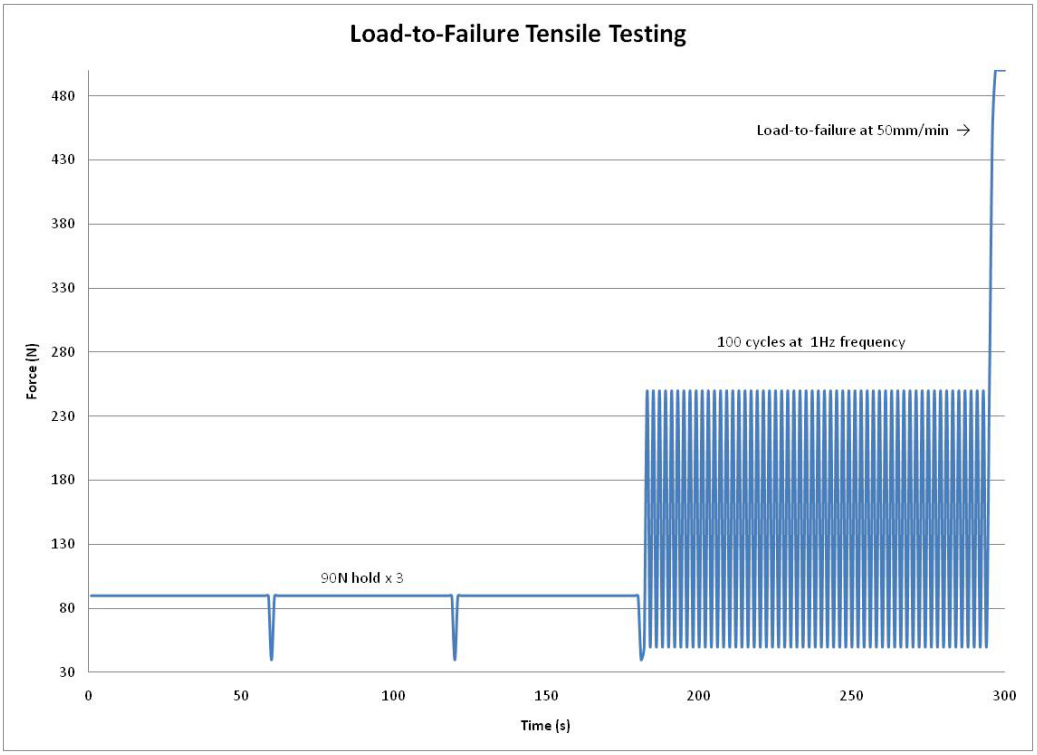

Figure 2-2. Load-to-failure test protocol.

Table 2-1. Practical difference values and standard deviation values for parameters in order to determine appropriate sample size at a power of 0.9.

Parameter	Practical Difference	Standard Deviation
UTF	700 N	606.84
UTS	26.82 MPa	28.30
UTε	0.14 mm/mm	0.034
E avg	191.57 MPa	0.38

CHAPTER 3
MATERIALS AND METHODS II

Marathon Test for Cyclic Loading

Tendon Preparation

Twenty samples were acquired from twelve donors for the marathon simulation. Only proximal ends were tested due to the grips for this test, and measurements were acquired in the same manner as for that of the load-to-failure test method. Tendon length between the grips for this test ranged from 16.08 mm to 35.7 mm with an average of 26.85 mm. This discrepancy was also due to the gripping method adopted for the marathon test; however, in dynamic testing, Young's modulus is not dependent on specimen length[29]. Also, AT tendons prepared for the marathon test were aseptically processed and were not sterilized through the BioCleanse© sterilization process. Again, this does not alter the viability of comparison amongst tendon samples according to Schimizzi et al[26].

Gripping Mechanism

The marathon simulation test was performed in a saline bath; therefore, the standard freezing method was not possible. Soft tissue grips with rough surfaces were initially used to grip the tendons; however, yield was not consistent with this method and tendons were being torn at the interface of the gripper. A grooved appliance designed to fit over the grip surface was next attempted, where the tendon would "snake" around the grooves. This method provided more consistent results, but the tendon sample was subjected to micro-tearing at the interface where it emerged from the grips. To mitigate this problem, a foam sheet was cut in the shape of the grooved appliance and served as

a protective barrier against rubbing at each end. This did not interfere with the response of the tendon to the applied forces.

Only the proximal end of the tendon was tested in the marathon test because of this gripping system. With the necessary tightness of the grip to prevent slippage and the "snaking" of the tendon, distal ends, which are more elliptical in shape, could not sustain their shape and failed at the grip interface. No problems were found with testing the more proximal ends of the tendons.

Test Method

The marathon test was also performed using the MTS 858 Bionix testing system, and Multiworks software recorded the time, extension, and force applied to the sample throughout the test. Parameters were selected for this marathon test to best simulate the impact that an ACL experiences during a 26.2 mi run for a competitive runner in vitro. Load values were calculated based on a runner with a mass of 55 kg, which was reported as the average mass of a top-class marathon runner by Billat et al[31]. Results from the top ten male and top ten female finishers of the Boston Marathon of 2009 were averaged to find the speed of the runners, and thus the stride length. A stride length of 3.60 m was calculated based on the reported race frequency of 1.37 Hz by De Zee et al[32] and average Boston marathon running times of 2 h and 22.6 min[33]. Race day preparation was also factored into the test protocol, which both simulated the race experience, and also served to precondition the tendon before exerting marathon forces and frequencies on the tendon. Ambulation with forces of 50 N to 250 N was first applied with a frequency of 0.67 Hz for 100 cycles as a warm-up to the marathon. Next, three 90 N holds of 30 s duration were applied, thus further preconditioning the tendon and simulating a stretch sequence by the runner. Finally, the marathon proceeded with

forces of 250 N to 600 N at a frequency of 1 Hz for the first 1000 cycles. The frequency was then increased to 1.37 Hz for the remaining 10,712 cycles of the marathon. The entire marathon test, including preconditioning, lasted about 2.5 hr. Maximum forces experienced by the ACL during running are estimated to be about 2.2 times bodyweight[34]. For a mass of 55 kg, the estimated load at peak impact of the ACL is 1191.3 N. This load was then divided in half to represent the load that would be experienced by one strand of a double-stranded graft. A picture of this test set-up is provided in Figure 3-1 and a plot describing the test protocol is provided in Figure 3-2.

To prevent desiccation of the tendon over the 2.5 hr period, the tendon was tested in a saline bath of 0.1% to 0.5% saline (salinity measured with an Accumex probe). Ideally, this salinity would have been maintained at physiological levels, which would have been closer to 0.6% salinity levels[35]. Because tendons are viscoelastic materials, temperature is an important factor. Water temperature for the marathon test was therefore maintained at the physiological level of 37ºC by using an immersion heater within the bath.

Calculations derived from the data collected included strain, strain rate, Young's modulus, extension, hysteresis, and dynamic creep. Strain was calculated as the change in length (extension) of the tendon over the original length of the tendon, and Young's modulus was calculated based on Hooke's law, where the slope of the linear portion of the stress-strain curve represented stiffness for each load and unload cycle component. The area between the load and unload curves of the stress-strain plot was calculated for hysteresis. Dynamic creep was found by calculating the difference

between the strain of the peak of the last cycle and the strain of the peak of the first cycle.

Statistical Methods

Marathon Test for Cyclic Loading. A sample size of 20 AT tendons was determined in order to achieve a representative response. Because 10 female and 10 male race results were used to calculate the test protocol, a sample size of 20 was selected. To analyze phenomenon within this group, Bartlett's test for equal variance was used, and a t-test with a 95% confidence interval was utilized. The marathon test method, however, was not designed as a comparative analysis.

Figure 3-1. Marathon test set-up with the MTS 858 Bionix testing system.

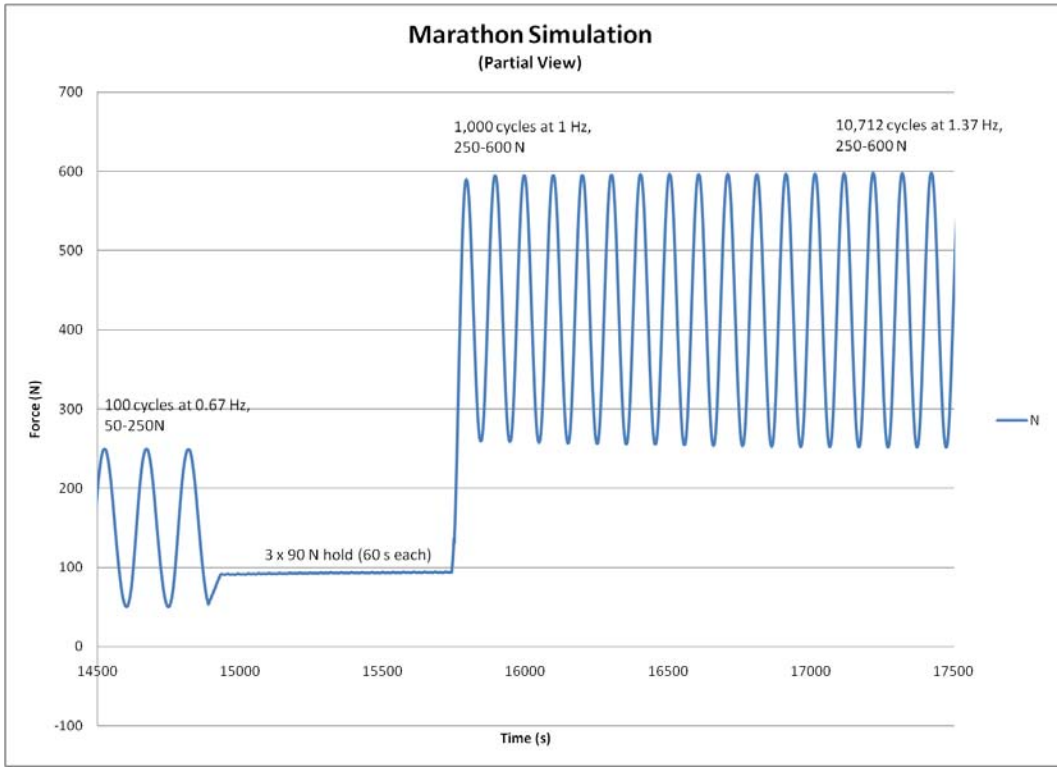

Figure 3-2. Marathon test protocol summary.

CHAPTER 4
RESULTS I

Load-to-Failure Test

Statistical comparisons of biomechanical results were first conducted to compare EDL, FDL, FHL, and PB separately as single strands. An independent evaluation of the four tendons, excluding AT, provided information concerning properties that cannot be simply doubled and also helps to determine which, if any, of the four smaller tendons possess specific qualities that are of special interest. Analysis was then conducted for all five tendons as single strands, and finally, a statistical comparison of double strand EDL, FDL, FHL, and PB compared to the single strand AT was conducted. Table 4-1 provides single strand biomechanical results of all tendons and Table 4-2 provides a hypothetical comparison of double strand EDL, FDL, FHL, and PB to the single strand AT. All p-value results are listed in Table 4-3.

Cross-Sectional Area of EDL, FDL, FHL, PB, and AT

The cross-sctional areas of the EDL, FDL, FHL, and PB were measured as single strands; however, according to the results of Hamner et al., the doubling of these values provides an approximation of the properties achieved for double stranded testing[10]. Average cross-sectional areas were measured at 8.85 mm^2, 9.88 mm^2, 11.97 mm^2, and 15.98 mm^2 for the tendons EDL, FDL, FHL, and PB, respectively. Unequal variance was found between the four tendons ($p << 0.05$); therefore, a Brown-Forsythe f-test was administered. The only tendons that were found to be statistically similar were EDL and FDL ($p > 0.05$). The average cross-sectional area of single strand AT tendons was measured at 26.10 mm^2, which is statistically greater than the assumed double strand

configuration of EDL, FDL, FHL, and PB ($p << 0.05$). Figure 4-1 displays average cross-sectional areas for each tendon.

Biomechanical Results of EDL, FDL, FHL, and PB

UTF. Average UTF values were 1136.5 ± 291.8 N, 954.1 ± 270.5 N, 1156.3 ± 348.0 N, and 1285.9 ± 300.0 N for the single strand tendons EDL, FDL, FHL, and PB, respectively (Fig 3-2). The average UTF value for AT was 2122.28 ± 574.68 N. Analysis of EDL, FDL, FHL, and PB showed that the UTF values had equal variance with a Bartlett's Test p-value of 0.496. One-way ANOVA for UTF showed a significant difference in the maximum loads ($p<<0.05$), with FDL displaying a different and lower UTF value according to Tukey's 95% simultaneous confidence intervals. Removal of FDL from the four-tendon cohort gave a p-value of 0.069, indicating no difference in UTF for EDL, FHL, and PB. Figure 4-2 displays average UTF values for EDL, FDL, FHL, and PB. When including AT into this analysis, unequal variance was detected and Brown-Forsythe analysis indicated that AT was statistically greater than EDL, FDL, FHL, and PB as single strand tendons ($p<<0.05$).

UTS. Average UTS values were 134.59 ± 36.0 MPa, 99.45 ± 25.9 MPa, 101.98 ± 28.9 MPa, and 87.85 ± 22.5 MPa for the tendons EDL, FDL, FHL, and PB, respectively. The average UTS value for AT was 91.05 ± 28.04 MPa. Comparing EDL, FDL, FHL, and PB, variances were found to be unequal according to Bartlett's test ($p=0.027$), and the Brown-Forsythe f-test indicated a difference between at least one pair of groups ($p=0.00064$). A Welch's t-test was then computed to find that EDL was significantly greater than all other tendons. Analysis of all five tendons gave the same results with EDL being statistically greater than all other tendons according to Tukey's 95%

simultaneous confidence interval. Figure 4-3 plots average UTS values for all five tendons.

Young's modulus. Average Young's modulus values were 1820.4 MPa, 1453.6 MPa, 1442.7 MPa, and 1220.3 MPa for the tendons EDL, FDL, FHL, and PB, respectively. The average Young's modulus value for AT was 1387.2 ± 487.5 MPa. Equal variances were found for the EDL, FDL, FHL, and PB comparison ($p=0.403$) but there was a significant difference in Young's modulus values for EDL compared to the other tendons according to Tukey 95% simultaneous confidence interval ($p<<0.05$).

When Young's modulus of elasticity was statistically analyzed against all five tendons, no difference in variance was detected ($p=0.075$). However, one-way ANOVA indicated that there was a significant difference amongst the five tendons ($p<<0.05$). Analysis with a Tukey 95% simultaneous confidence interval showed that EDL, again is significantly greater than all other tendons. Figure 4-4 displays the average Young's modulus values for all five tendons. Additionally, Figure 4-5 displays average Young's modulus values across 100 cycles of the test protocol.

Strain. Average strain values were 0.107 mm/mm, 0.0960 mm/mm, 0.103 mm/mm, and 0.113 mm/mm for the tendons EDL, FDL, FHL, and PB, respectively. These tendons displayed equal variance values ($p=0.654$), but one-way ANOVA indicated a difference between FDL and PB. A Tukey 95% simultaneous confidence interval showed that PB had a significantly greater strain than FDL.

Strain was calculated for AT as 0.11 ± 0.033 mm/mm. Statistical analysis displayed that there was unequal variance amongst the tendon cohorts and further analysis showed a statistical difference amongst the tendons ($p=0.033$) with PB having

a greater strain than FDL and AT having a greater strain than both FDL and FHL according to Welch's t-test. Figure 4-6 displays average strain values for each tendon.

Extension: Average extension values during the load-to-failure were 3.75 mm, 3.35 mm, 3.60 mm, and 3.96 mm for the tendons EDL, FDL, FHL, and PB, respectively. Equal variance ($p=0.677$) allowed for a one-way ANOVA test, which indicated that at least one value was different ($p=0.015$). Further analysis applying a Tukey 95% simultaneous confidence interval showed that PB had significantly greater extension than FDL.

Average extension was recorded for AT as 4.05 ± 1.18 mm. Comparison of extension against all tendon cohorts did not display equal variance according to Bartlett's test ($p<<0.05$), therefore, a Brown-Forsythe f-test was again executed to detect for any differences within the tendon cohorts, and it detected that there was a difference between at least one pair of tendons ($p=0.031$). Using a Welch's t-test, it was determined that PB had a statistically greater extension than FDL, and AT had a statistically greater extension than FDL and FHL. Figure 4-7 displays average extension values for each tendon.

Assumed Double-Strand Comparison

Single strand UTF values for EDL, FDL, FHL, and PB were doubled for each sample to conjecture how these tendons would compare to a single strand AT, which is currently an accepted allograft tissue. This double strand comparison mimics the current double strand gracilis and semitendinosus allograft combination.

The average single strand AT tendon is 2122.2 N, and the assumed double UTF for the four tendons was calculated as 2273.0 N, 1908.2 N, 2312.6 N, and 2571.7 N for the EDL, FDL, FHL, and PB tendons, respectively. Equal variance produced a p value

of 0.574 and one-way ANOVA utilizing a Tukey 95% simultaneous confidence interval indicated that a doubled PB is significantly higher than the single strand AT ($p<<0.05$). Figure 4-8 displays UTF values with double strand EDL, FDL, FHL, and PB, and single strand AT.

Table 4-1. Single strand average biomechanical results for EDL, FDL, FHL, and PB

Tendon	UTF (N)	UTS (MPa)	E* (MPa)	UTε (mm/mm)	n
EDL	1136.5 ± 291.79	134.6 ± 35.98	1820.4 ± 0.45	0.11 ± 0.024	36
FDL	954.1 ± 270.46	99.5 ± 25.94	1453.6 ± 0.38	0.096 ± 0.023	36
FHL	1156.3 ± 347.99	102.0 ± 28.88	1442.7 ± 0.47	0.10 ± 0.022	36
PB	1285.9 ± 300.03	87.9 ± 22.46	1220.3 ± 0.37	0.11 ± 0.03	44

*E represents Young's modulus.

Table 4-2. Average biomechanical results of double EDL, FDL, FHL, and PB and single AT

Double Strand	Max Load (N)	UTS (MPa)	CSA (mm^2)
double EDL	2272.98	128.42	17.70
double FDL	1908.16	96.57	19.76
double FHL	2312.56	96.60	23.94
double PB	2571.72	80.47	31.96
single AT	2102.68	86.09	26.10

Table 4-3. Statistical analysis of all cohort groupings.

Cohort	Parameter	Bartlett's test	ANOVA/Browne-Forsythe	Tukey's 95% CI/Welch's t-test
4 tendons*	UTF	0.496	0.00	FDL different from EDL, FHL, and PB
	UTS	0.027	0.00064	EDL > all
	E	0.40	<< 0.05	EDL > all
	ε	0.65	0.015	PB > FDL
	Ext	0.68	0.015	PB > FDL
5 tendons†	UTS	0.057	<< 0.05	EDL > all
	E	0.075	<< 0.05	EDL > all
	ε	<< 0.05	0.033	PB>FDL, AT>FDL,FHL
	Ext	<< 0.05	0.031	PB>FDL, AT>FDL,FHL
Double Strand‡	UTF	0.57	<< 0.05	dbl PB>single AT
	UTS	0.017	0.0020	single AT> dbl PB

*4 tendons: EDL, FDL, FHL, and PB. †5 tendons: EDL, FDL, FHL, PB, and AT. ‡Double strand: double EDL, FDL, FHL, and PB compared to single AT.

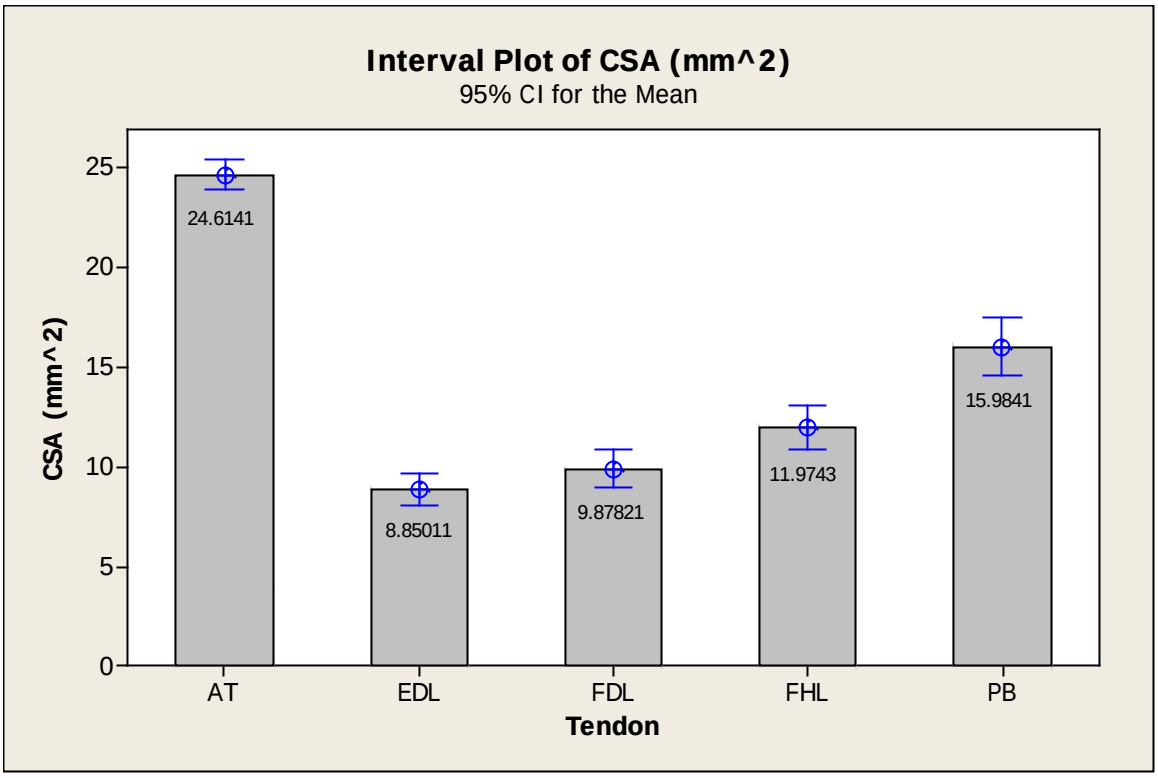

Figure 4-1. Average cross-sectional area (CSA) of each tendon.

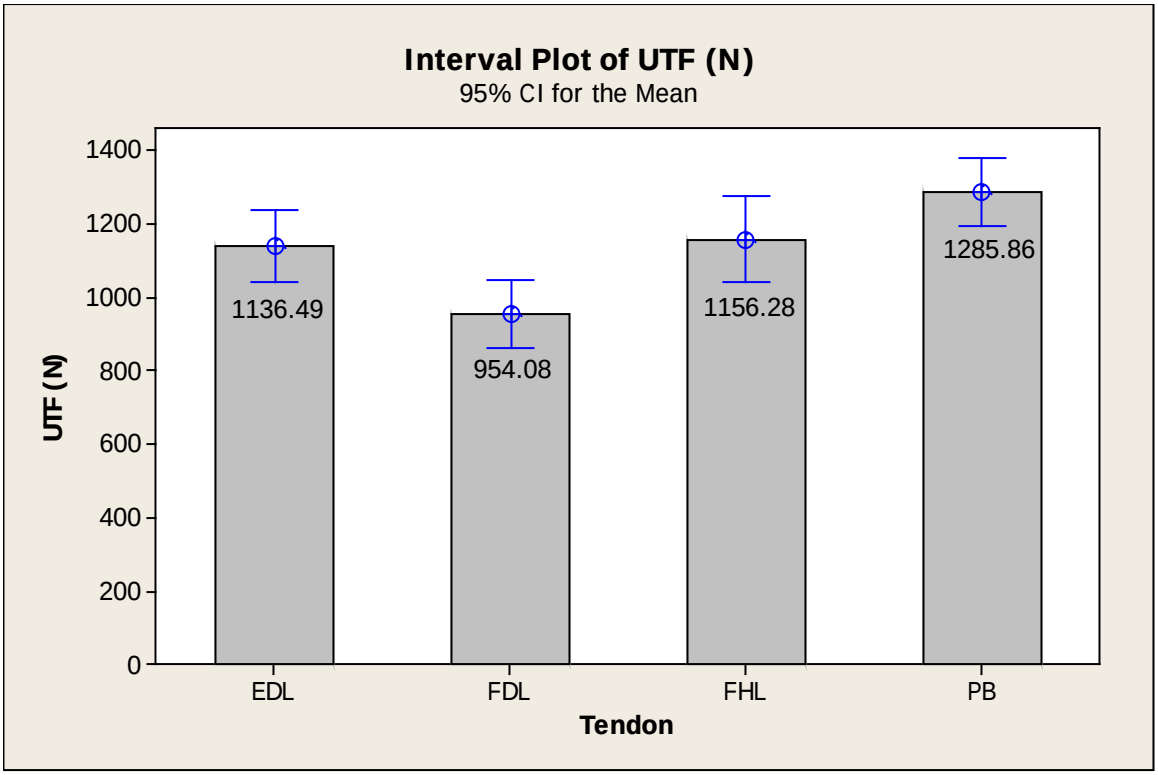

Figure 4-2. Biomechanical UTF results for EDL, FDL, FHL, and PB.

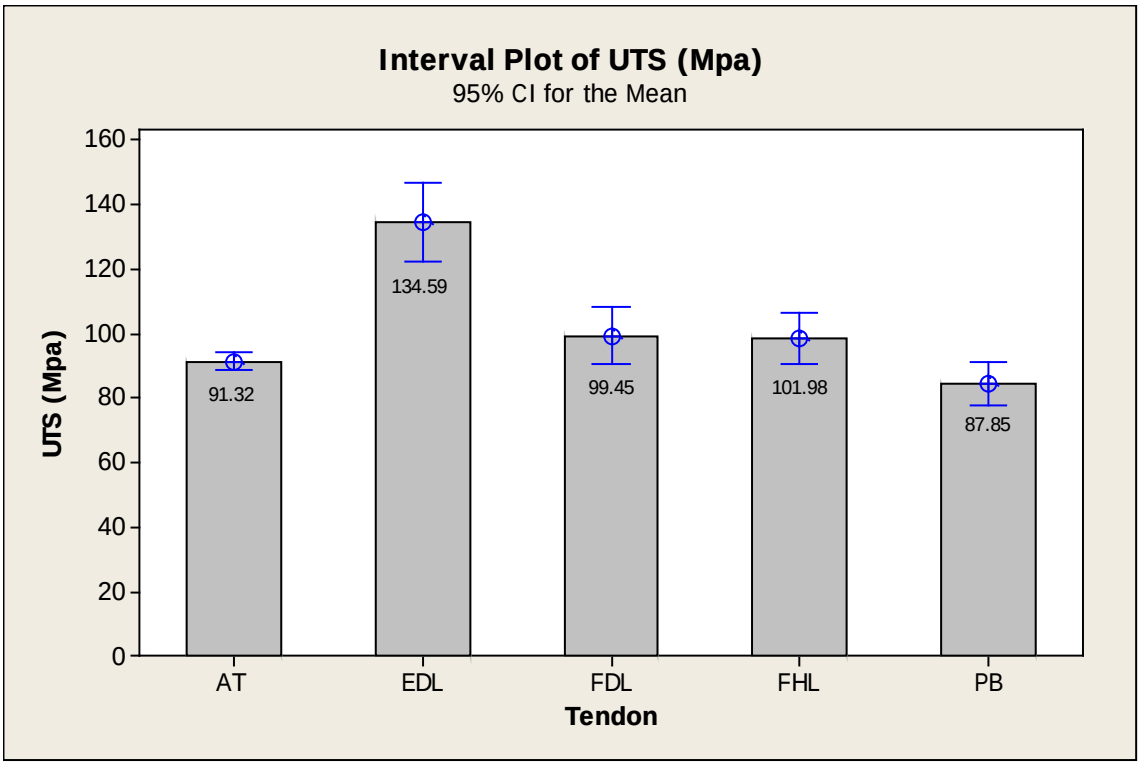

Figure 4-3. Biomechanical UTS results for single strand AT, EDL, FDL, FHL, and PB.

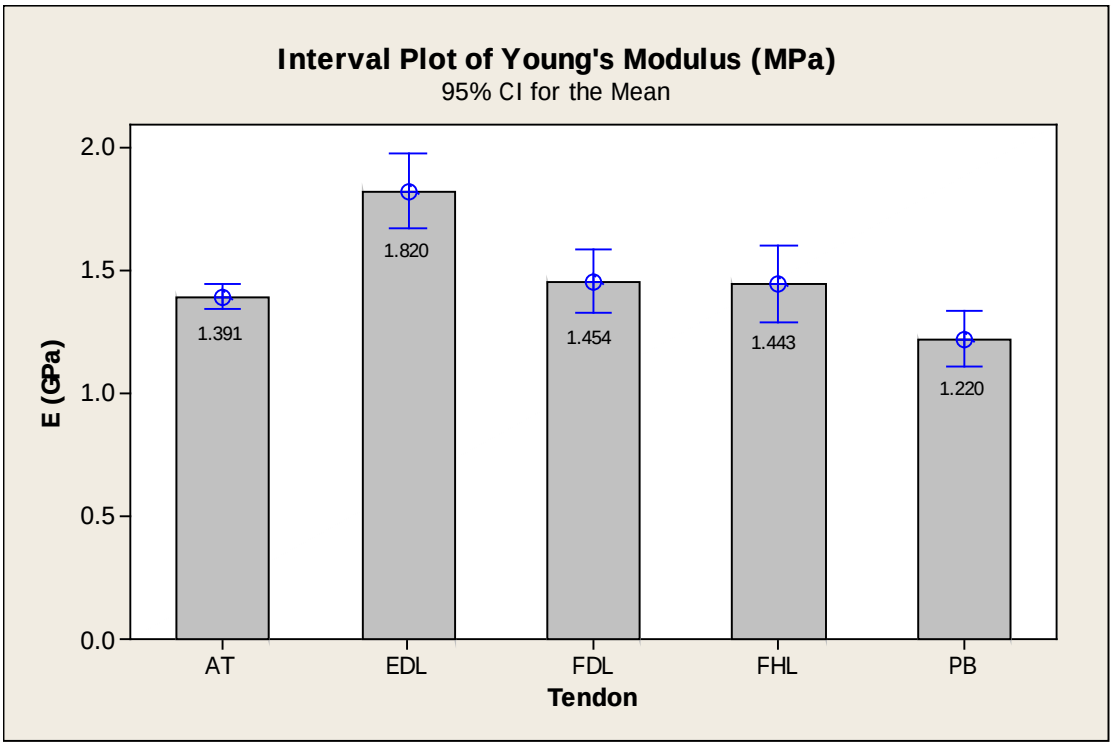

Figure 4-4. Biomechanical Young's modulus results for single strand AT, EDL, FDL, FHL, and PB.

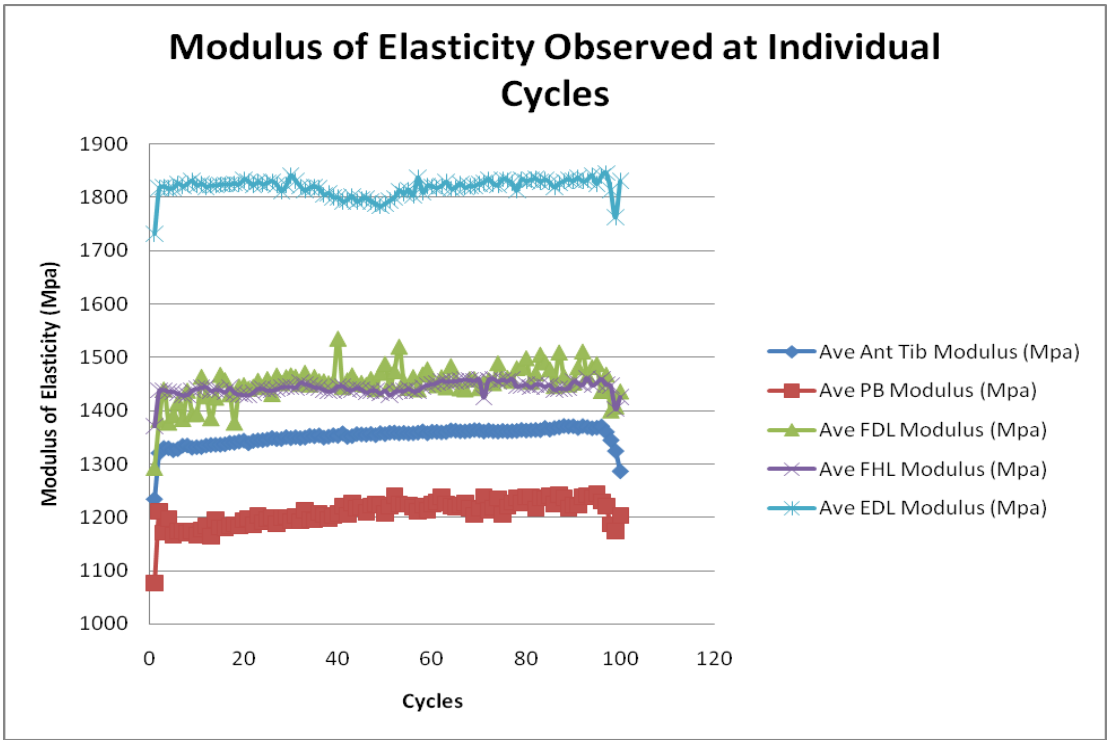

Figure 4-5. Young's modulus averaged for each tendon over 100 cycles.

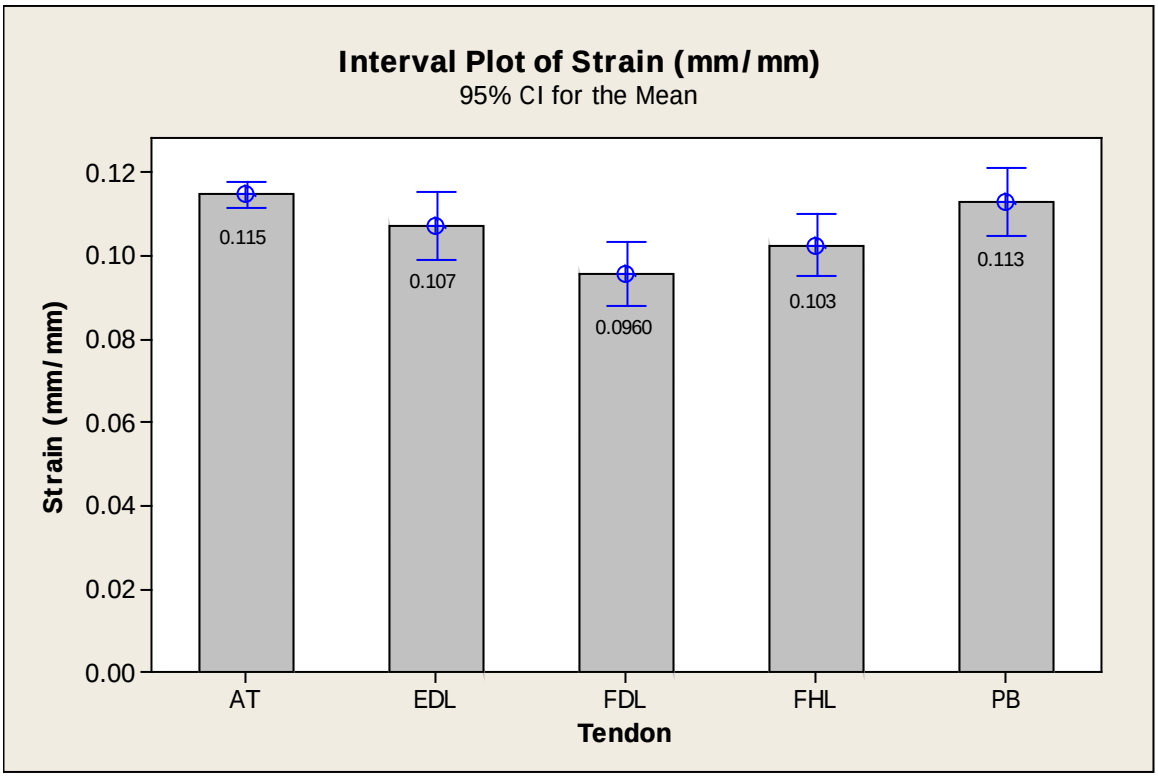

Figure 4-6. Biomechanical UTε results for single strand AT, EDL, FDL, FHL, and PB.

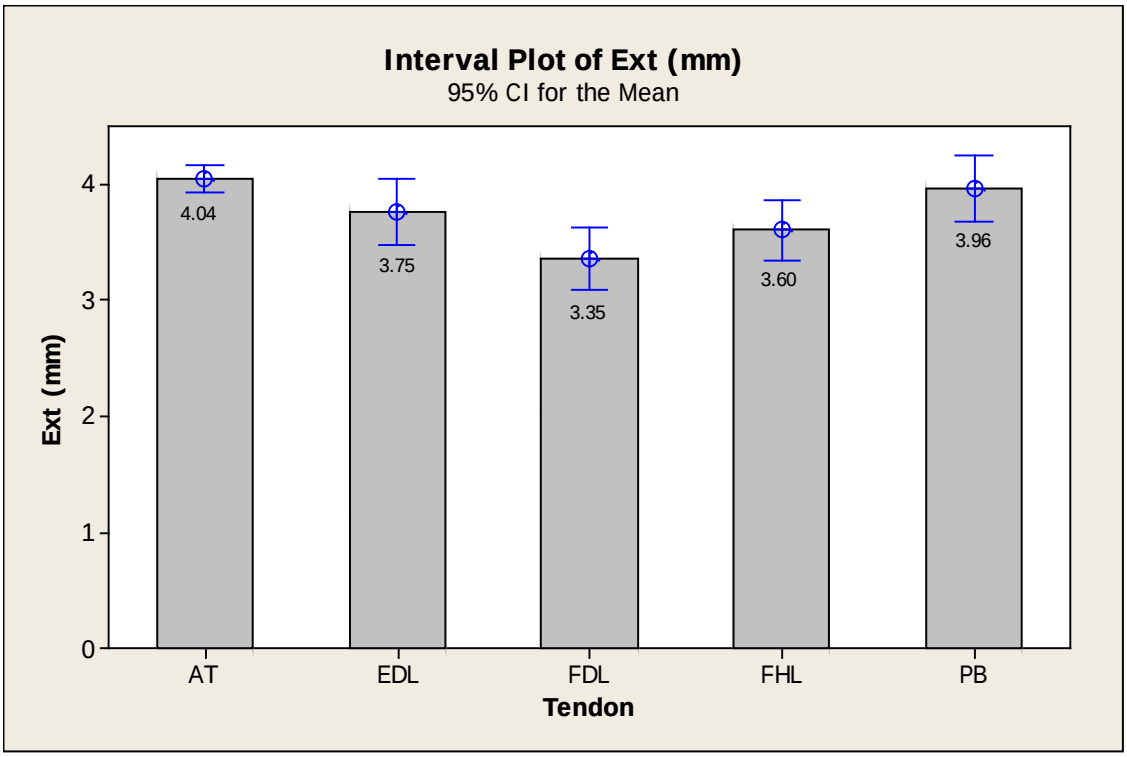

Figure 4-7. Biomechanical UText results for single strand AT, EDL, FDL, FHL, and PB.

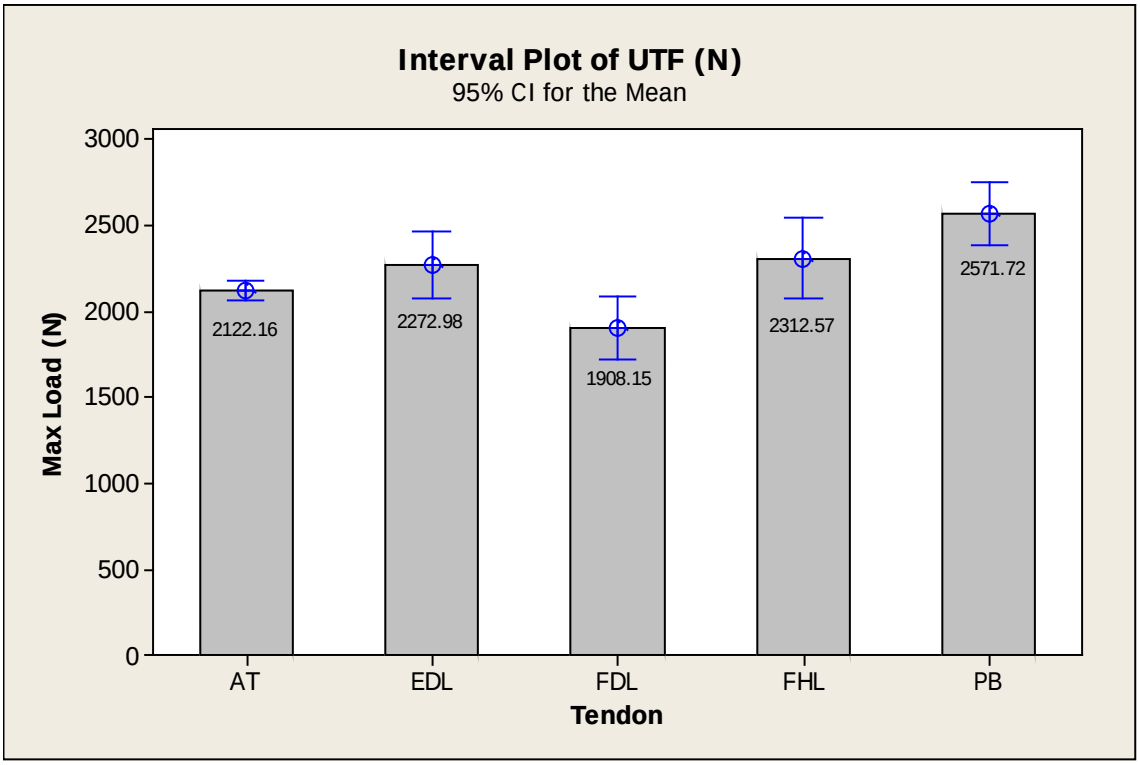

Figure 4-8. Biomechanical UTF results for double strand EDL, FDL, FHL, and PB compared to single strand AT.

CHAPTER 5
RESULTS II

Marathon Test for Cyclic Loading Test

Average AT cross-sectional area values for the marathon test ranged from 20.49 mm^2 to 43.84 mm^2, and the average cross-sectional area was 31.18 mm^2. Density measurements were taken at room temperature and an average of 0.95 g/ml was calculated, with a range of values between 0.802 g/ml and 1.163 g/ml. This is very close to the density of water, which is about 1g/ml at room temperature.

Biomechanical Results of AT under Dynamic Loading

Properties averaged over data derived from the entire marathon test were calculated, such as dynamic creep, average strain, average extension, average Young's modulus, and average stress. These values were also determined after 1000 cycles, a half marathon, and a full marathon, and this information is located in Appendix A, which also includes a table relating the load and unload values at these three time points. The parameters of strain, extension, Young's modulus, and hysteresis were also plotted and observed for changes over time as the test progressed and the tendon was subjected to elements of fatigue. Regression line equations of each tendon sample for these parameters are included in Appendix B.

Dynamic creep. Dynamic creep is the difference of the strain of the last cycle peak and the strain from the first cycle peak. The average dynamic creep of all twenty marathon tests was 0.0780 ± 0.039 mm/mm, with a range of 0.0152 mm/mm to 0.151 mm/mm. The average dynamic creep of tendons exhibiting tertiary creep (loss of stiffness) was 0.063 mm/mm (n=7), and the average dynamic creep of tendons

exhibiting primary creep (no loss in stiffness) was 0.086 mm/mm (n=13). Figure 5-1 shows the dynamic creep of a sample specimen.

Strain. Strain values remained in the physiological range with a minimum average strain of 0.106 mm/mm and a maximum average strain of 0.465 mm/mm. The average strain over the course of the marathons was 0.279 ± 0.118 mm/mm. Figure 5-2 indicates a positive slope for increasing strain over time. All of the samples in the marathon exhibited positive slopes indicating increasing strain as the marathon test progressed. However, strain rate was found to decrease as the test progressed.

Extension. Average extension of the tendon over the duration of the marathon was 6.88 ± 1.93 mm, with a range of 3.45 mm to 11.38 mm. Extension over the duration of the 11,712 cycles was logarithmic with a positive slope, indicating that the tendon was still extending at the end of the cycles and had not reached a state of equilibrium. Figure 5-3 shows the extension at minimum load, maximum load, and average load.

Young's modulus of elasticity. The average Young's modulus for the duration of the marathon was 382.04 ± 133.16 MPa. The range for all twenty marathons was 168.485 MPa to 626.897 MPa. Seven of the marathons had a final negative slope, indicating that by the end of the cycling, the stiffness of the tendon was decreasing. The remaining thirteen tendons increased in Young's modulus values as the cycle number increased, indicating stress hardening of the tendon. The frequency increased from 1 Hz to 1.37 Hz at cycle number 1000, and an evident increase in Young's modulus occurred at this increase in frequency and then the tendon returned to its previous Young's modulus trend. At cycle 1000, the Young's modulus of Fig 5-4 is

361.35 MPa and increases to a maximum Young's modulus value of 370.31 MPa at cycle 1003. The Young's modulus value then continues to decrease and falls below its 1000 cycle value of 361.35 MPa at about cycle 9300. The gradual decrease of Young's modulus after the increased frequency could be tendon recovery, or it could indicate fatigue of the tendon over time. This result is consistent, however, with Schechtman et al's conclusion that frequency does not cause any discernable trends on the dynamic parameters of tendons in loading[36].

Hysteresis: Measurements were calculated to determine the hysteresis by taking into account the load and unload areas of the stress-strain curve. Rebound resilience accounts for the energy not dissipated by the effects of hysteresis. Finally, the rate of hysteresis was also determined. The average hysteresis during the course of the marathon was 0.0515 ± 0.0124; therefore, the average rebound resilience 0.949 ± 0.0124. The range for hysteresis was 0.0304 to 0.0733 and the range for rebound resilience was accordingly 0.927 to 0.970. Hysteresis was found to decrease over time with a minimal negative slope as the tendon became stiffer and the area between the stress-strain curve decrease (Figure 5-5 and Figure 5-6). The average rate of hysteresis was calculated as 2.35E-5 s^{-1}, and steady state of hysteresis was assumed after analyzing that hysteresis values were greater than 98% percent consistent from mid-marathon to the end of the marathon.

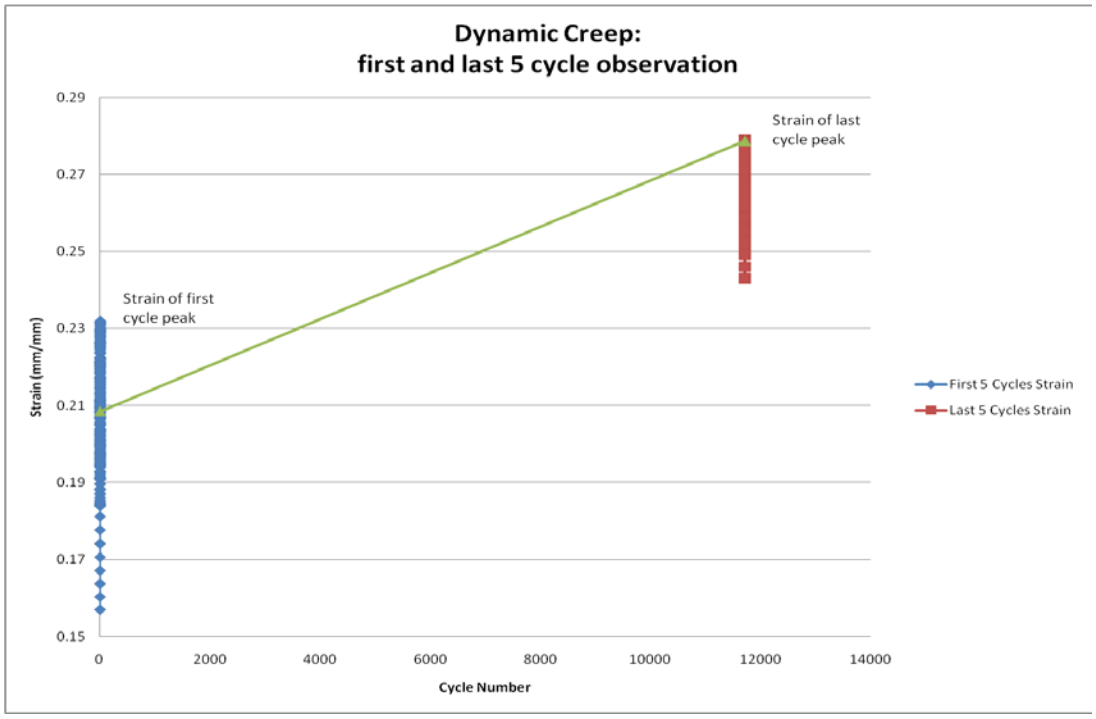

Figure 5-1. Dynamic creep. The peak strain of the first cycle and the peak of the last cycle are plotted to show dynamic creep.

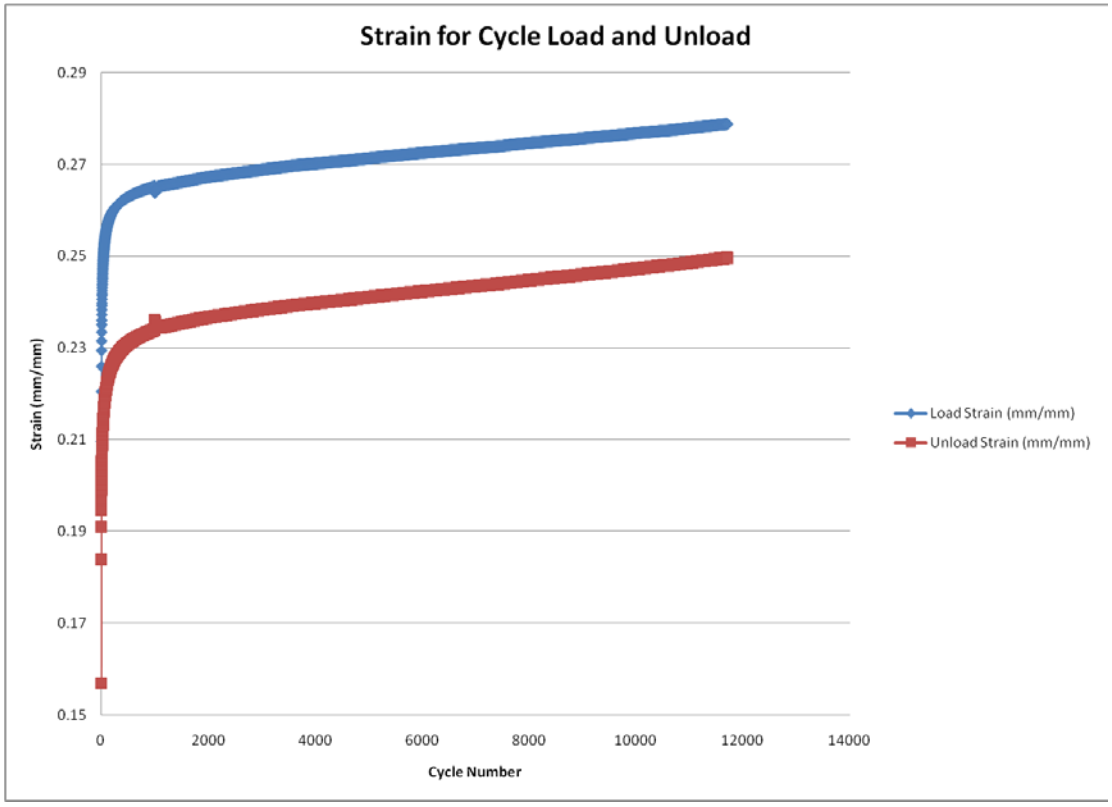

Figure 5-2. Strain. Load cycles exhibit higher strain than unload cycles.

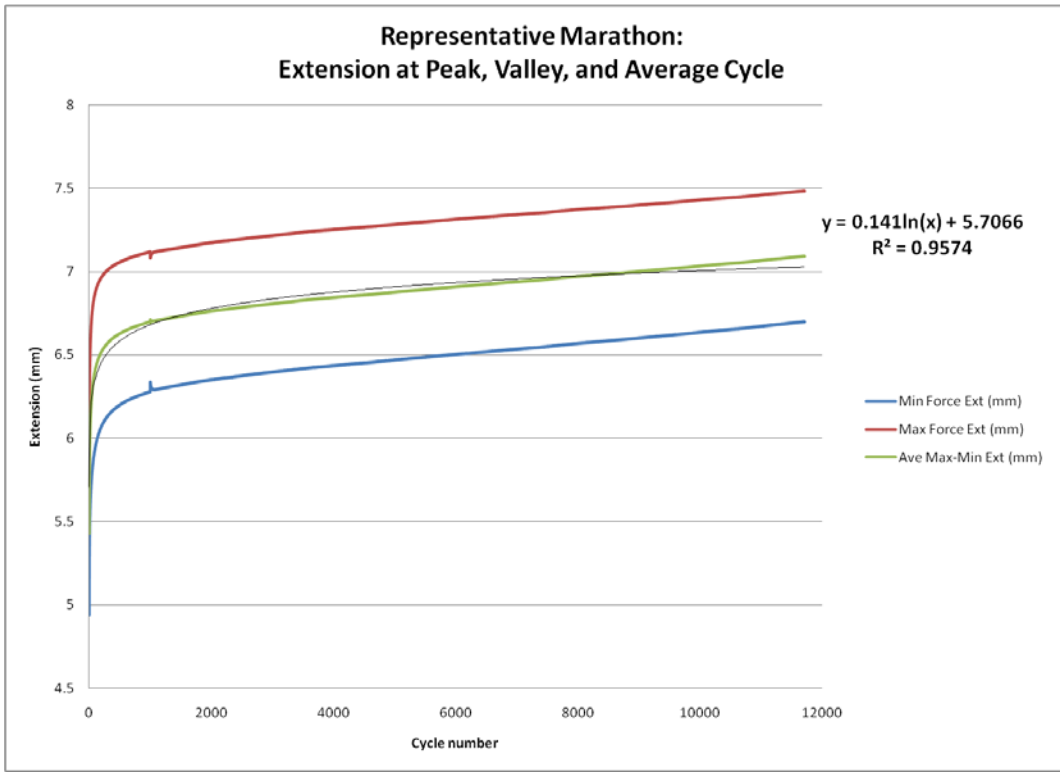

Figure 5-3. Extension at maximum, average, and minimum loads.

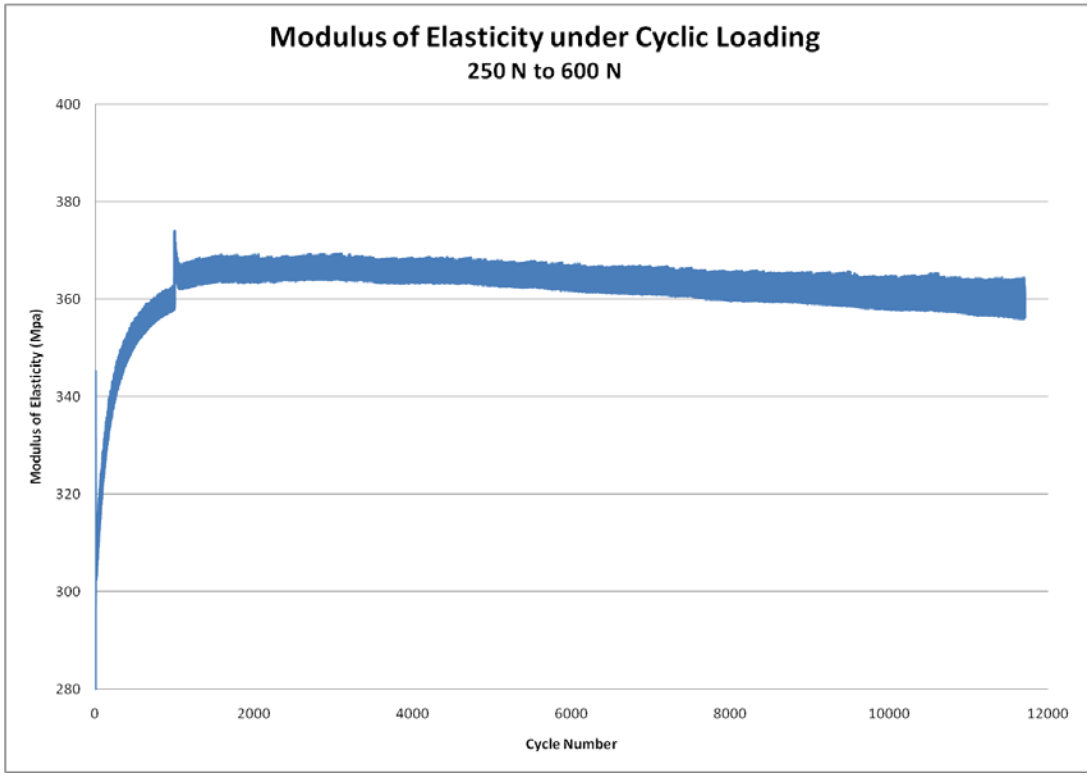

Figure 5-4. Young's modulus. Average load and unload cycles plotted.

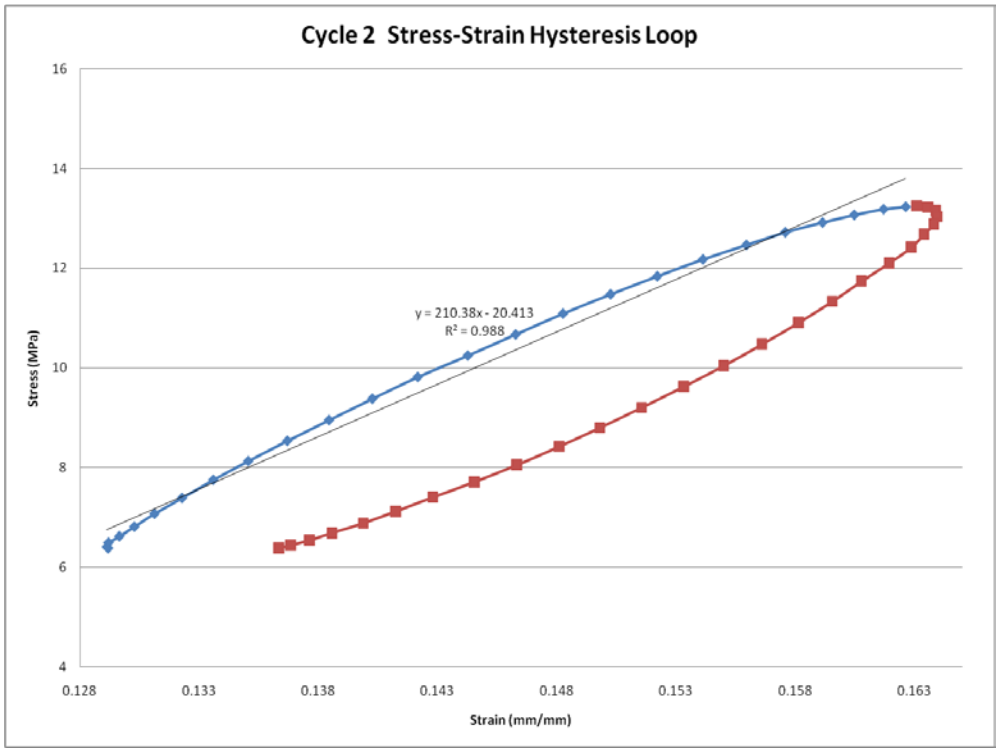

Figure 5-5. Cycle 2 stress-strain curve displaying hysteresis as the area between the curves.

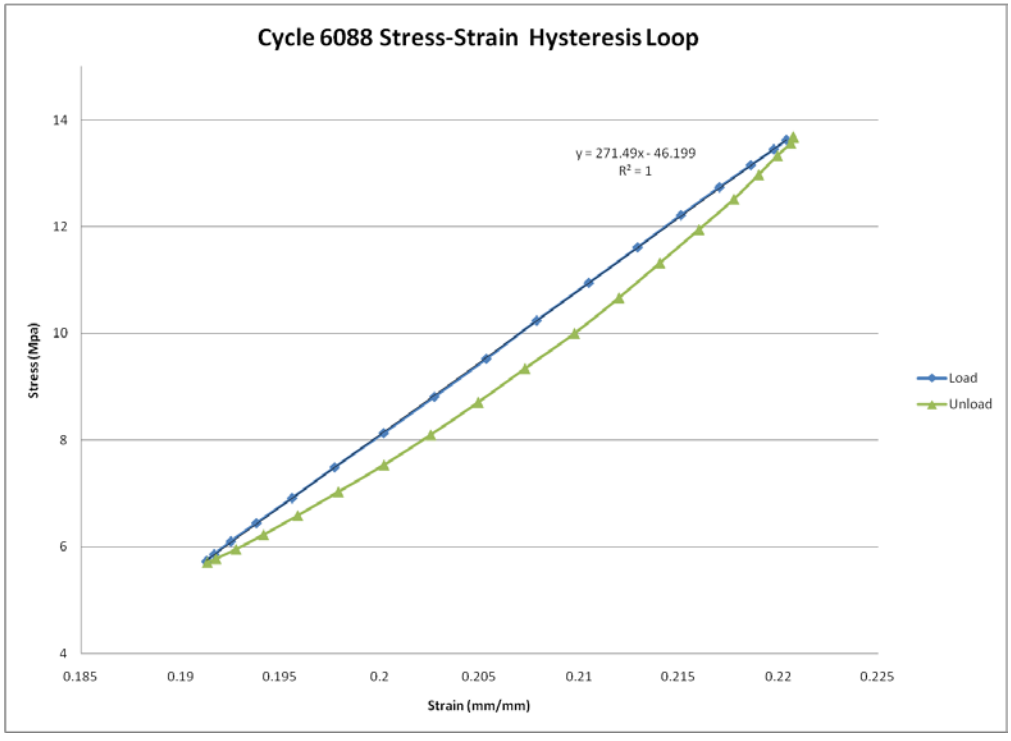

Figure 5-6. Cycle 6088 stress-strain curve displaying hysteresis as the area between the curves.

CHAPTER 6
DISCUSSION I

Load-to-Failure Test

Biomechanical testing of the EDL, FDL, FHL, and PB provided results that are positive and promising for future use as allograft material. The inclusion of the four tendons EDL, FDL, FHL, and PB to the retinue of currently accepted allografts provides up to four times more grafts per donor. The four tendons were described as double strand assuming matching tendon type; however, combinations of the tendons are also capable of being paired. AT, as has been reported previously, also displayed efficacious biomechanical results as an ACL replacement graft, both as a single strand and as a double strand. The mechanical performance inherent in any particular tendon results from the load patterns it experiences and the subsequent fibril size that develops as a response to these stresses[37].

Biomechanical Attributes

Comparing single strand UTF values amongst the four tendons resulted in a significant difference between FDL, EDL, FHL, and PB, with FDL having a lower value of 954.1 N. This value, however, is still higher than the determined practical difference of 700 N. Even as a single strand, this tendon would sustain the estimated forces experienced by the ACL during normal activity[11,14,17,18]. When doubled, EDL, FHL, and PB all displayed a higher UTF than the single stranded AT. Statistically, doubled EDL, FDL, FHL, and PB are all viable ACL replacements when compared to the currently accepted single strand AT tendon. Additionally, all four of the smaller tendons displayed greater average UTF values than the gracilis tendon, as reported by both

Hamner et al. and Noyes et al.[10,18], and all but the FDL tendon are within the range of UTF values reported in these two studies for the semitendinosus tendon[10].

UTS values provide a more normalized description of the strength of the tendon because they take cross-sectional area into account. This parameter displays that FDL, FHL, and PB were not different from AT in UTS values, and EDL was in fact significantly greater than AT. The cross-sectional area of EDL is the smallest of all of the tendons, being only about 34% that of the AT tendon, and the FDL, FHL, and PB tendons are about 38%, 46%, and 61% that of the AT cross-sectional area, respectively. Given the small size of the four tendons in relation to that of the AT tendon, this indicates that fibril distribution of the smaller tendons is more dense[37]. Implant site morbidity is reduced when smaller tunnels are required for implantation, as would be the case in utilizing the smaller tendons EDL, FDL, FHL, and PB, which provide the same or greater mechanical strength as other allografts.

The muscle to which each tendon is associated and its function determine the strain necessary to complete each task, whether responsible for fine movements, extension, or flexion. A greater strain value would prevent the tendon from impeding fine movement and would signify greater elongations during loading[38]. The similarity of strain between all five tendons is expected, given the location of the tendons in the lower leg and their function to aid in steadying the tibia and fibula perpendicularly on the talus. While there were statistically different strain values amongst different tendons, these differences were practically insignificant (no greater than 0.14 mm/mm). As would be expected, increased strain values displayed a relationship to decreased values of Young's modulus.

Young's modulus indicates the degree to which the tendon stores and reuses elastic energy according to its function[38]; therefore, stiffer tendons exhibit greater Young's modulus values and do not utilize elastic energy with the same efficiency as a tendon with a lower Young's modulus value[39]. The stiffest tendon was EDL, with a statistically greater Young's modulus than any of the other tendons. This tendon branches into four strands as it approaches the digits of the foot and may need to be stiffer in order to maintain its integrity as it separates and terminates at each digit. Young's modulus values for EDL were reported by Schechtman et al. at values of about 1090 MPa to 1356 MPa[36], which is lower than the 1,820 MPa, value achieved with the load-to-failure test. FHL and FDL originate from the fibular and tibial sides of the leg, but in the sole, the FHL passes from the lateral to the medial side and is situated above FDL, where the two tendons are connected by a fibrous slip. This orientation exposes both tendons to the same mechanical stresses, and explains the similarity in Young's modulus response to cycling. PB was not statistically different from the tendons, excluding EDL, but it did provide the lowest Young's modulus value of all of the tendons at 1220 MPa. The function of the peroneus muscles is to steady the foot upon the leg, and thus a lower Young's modulus makes the tendon more compliant in this task.

CHAPTER 7
DISCUSSION II

Marathon Simulation Test

The marathon simulation replicated the forces experienced by the ACL during a long-term, high intensity run. The average stress subjected during the marathon was about 14 MPa, and this stress represented the forces experienced by one strand of a double strand implant. If the full impact of a 2.2 times body weight load[34] had been administered to a double strand AT tendon, the stresses would have remained the same because doubled forces would have also been matched with doubled cross-sectional area. All twenty of the tendons performed the marathon test without failure and the data that was collected from each specimen was useful in understanding the mechanisms that occurred as the tendon experienced long-term cyclic loading.

Biomechanical Attributes

Responses of strain, extension, Young's modulus, and hysteresis all possessed logarithmic trends, and each property displayed a spike at the 1000 cycle in response to the increased frequency. The stiffness of the tendon, or Young's modulus, is the best predictor of the state of damage accumulation in the tendon over time. Increasing stiffness, as seen in 13 of the 20 samples, indicated stress hardening as the tendon responded to the cyclic loading and stored more energy. Seven tendons, however, displayed negative slopes at the end of the marathon, thus indicating damage accumulation as stiffness was not maintained. While some tendons did display damage due to cyclic loading, they were still able to withstand cyclic loading without failure, indicating that the fibril network was not compromised beyond a state that could perhaps be reparable in vivo at the end of the marathon. Schechtman et al. observed

human tendons under the microscope after performing cyclic fatigue testing, and he reported that partially fatigued tendons displayed well aligned fibers forming a well organized microstructure[36].

The strain sustained by the AT tendons during the marathon simulation increased over time, but the strain rate was negative and practically steady-state. While increasing strain values would eventually lead to failure of the tendons in vitro, the incidence of a constant strain rate indicates that the tendons were able to sustain cyclic loading for the entire marathon. If cycling had been administered beyond the marathon duration, observation of increased strain and increased strain rate could act to predict failure. Wren et al. cyclically tested Achilles tendons to failure and reported that rapidly increasing strain rates were usually observed prior to tendon failure in cyclic loading[6]. Again, this verifies that the AT marathon tendons were sustaining the marathon loading pattern with only signs of fatigue and no signs of failure. No correlations were found between the average strains experienced by the tendons and the presence or absence of damage accumulation. Appendix C provides a plot of average strain and average Young's modulus values. Tendons that experienced damage are indicated on this plot.

Dynamic creep of the AT tendon during the marathon test averaged at 0.078 ± 0.039 mm/mm. A relationship between the overall average Young's modulus value and the dynamic creep value indicated that stiffer tendons produced less dynamic creep and more compliant tendons allowed the tendon to experience more dynamic creep. Of the twenty AT tendons tested in the marathon test, seven displayed tertiary creep, as indicated by a decrease in Young's modulus over time. The average dynamic creep of the tendons that did not exhibit tertiary creep (i.e. primary creep) was 0.086 mm/mm

(n=13) and the tendons that did exhibit tertiary creep had dynamic creep values of 0.063 mm/mm (n=7); therefore, the dynamic creep value is not an indicator of damage as much as the display of a loss of stiffness in the tendon. De Zee et al. modeled the response of an Achilles tendon to predict its dynamic creep during a marathon by conducting cyclic loading of 1600 cycles under the prescribed conditions experienced in running[32]. He assumed that 1600 cycles provided a representative tendon response because it was found that most of the dynamic creep occurred within this first period before reaching an asymptote[32]. According to the results of the author's present marathon test, greater than 1600 cycles are required to predict tendon response to long-term cyclic loading because of the effects of damage accumulation.

The viscoelastic property of hysteresis was examined to determine the energy dissipation of the tendon over time. Hysteresis and hysteresis rate both decreased over time, but this decrease was of 10^{-5} to 10^{-3} magnitude, indicating that hysteresis basically reached a steady state (less than 1.2% change from mid-marathon to the end of the marathon). Both hysteresis and Young's modulus values are derived from the same stress-strain relationship, but Young's modulus appears to increase or decrease with time, and the hysteresis response remained constant. Further analysis of modulus and hysteresis revealed that, over time, the stiffening of the tendon reached a point where no energy was dissipated and the tendon basically acted as an elastic solid. At the beginning of the marathon test, individual load and unload cycles plotted for stress-strain relationships displayed a hysteresis loop with a large amount of hysteresis, as indicated by the area between the curves. However, cycles analyzed at the end of the marathon test displayed load and unload stress-strain curves with little or no hysteresis.

During an in an vivo cycling test with human subjects, Kubo et al. found no significant correlations between hysteresis and stiffness, and he therefore deduced that the stiffness of the tendon did not affect the ability of the tendon to re-use elastic energy and recover lost energy due to internal damping[39]. The author's present study produced a similar result where little correlation was found between stiffness and hysteresis for the overall marathon, but correlation was detected for part of the marathon up to the point when the tendon started to display purely elastic properties.

The variation that was detected between different test specimens was expected because many factors contribute to tendon performance. Increased age is associated with decreased Young's modulus values[17], but this relationship was not directly indicated amongst the 20 specimen samples. Instead, in vivo mechanical loading of the tendon by the donor is thought to contribute to its performance in vitro[40]. Pike et al. studied high- and low- stressed sheep tendons and found that tendons which are subjected to high-stress during growth are more resistant to damage due to cyclic fatigue[37]. Reeves et al. performed a clinical study by incorporating strength training to fourteen elderly individuals for 14 weeks and found that exercise training increased patella tendon stiffness by 64% and reduced hysteresis by 28%[41]. These changes in stiffness and hysteresis are most likely due to increased packing density of collagen fibrils and changes in the collagen crimp structure[41]. If the activity level of the donors utilized in the marathon simulation test were known, it would be suspected that the tendons displaying damage accumulation belonged to less active individuals and the robust test tendons belonged to active individuals.

CHAPTER 8
TEST COMPARISONS: ATTRIBUTES, LIMITATIONS, AND FUTURE WORK

Viscoelastic Properties

Viscoelastic properties of the AT tendon were quantified with both test methods, load-to-failure and marathon simulation, and the factors that affected viscoelasticity were also thus quantified. Utilization of the same tendon type, AT, for both test methods allowed for direct comparison of environmental effects and greater discernment concerning tendon properties and sensitivities, with Young's modulus being the mode of comparison.

The average Young's modulus calculated for AT during the 100 cycles of the load-to-failure test was 1387.2 ± 487.5 MPa. However, the average Young's modulus value calculated for AT in the simulated marathon test was 382.04 ± 133.16 MPa. Due to the variations in the Young's modulus values reported in literature, it is apparent that test method imposes critical factors that influence the stiffness of the tendon[15,20,25]. To validate the responses calculated for each test, a load-to-failure test was performed with one of the marathon AT tendon samples. The marathon test was nondestructive, and after testing, this sample was frozen at -70ºC until further load-to-failure testing. The average Young's modulus value for this sample during the marathon test was of 505.6 MPa, but interestingly, when this same tendon was tested under different environmental conditions in the load-to-failure test, its Young's modulus was 1566.4 MPa. The UTF found for this tendon was 2613.6 N, which indicates that any damage which the tendon might have sustained did not affect its strength or stiffness.

With this comparison, it was deduced that parameters of the test method were responsible for this variation in Young's modulus. The factors that were not consistent

for each test included preconditioning parameters, frequency, applied force, temperature, and hydration of the tendon. To evaluate the potential effects of force and Young's modulus, the first ten cycles of the marathon test at a load profile of 50 N to 250 N and a frequency of 0.67 Hz was compared to the load profile of 250 N to 600 N and frequency of 1 Hz. The resulting Young's modulus values were 343.7 MPa and 534.2 MPa, respectively. This indicates that the tendon became stiffer in response to higher forces and an increased frequency. Also, the load profile of 250 N to 600 N occurred later in the test, so the tendon fibers might have aligned (preconditioned) at this point to work in concert. The first ten cycles of the load-to-failure test (1 Hz frequency and loads of 50 N to 250 N) for both AT and FDL were next compared to these marathon cycle Young's modulus values and the load-to-failure test consistently displayed greater Young's modulus values. Appendix D displays a table with summary results of 10^{th} cycle performance of tendons in the different tests.

Hydration of the tendon was first investigated to determine the mechanisms experienced by the tendon in both an immersed state and in a state exposed to air. Tendon hydration effects have been well documented[22,42-45], but hydration of the tendon is not often a focus of the test method because of difficulties that exist in gripping the tendon without slippage. The tendon in the marathon test was fully immersed, while the tendon in the load-to-failure test was frozen to its grips with warm tubing wrapped around the mid-substance of the sample for about 11 to 15 minutes and then it was tested for 5 minutes (~20 min without active hydration but with tubing protecting against evaporation). According to Han et al, changes in the apparent diffusion coefficient have a mean time of approximately 15 minutes; therefore, it is possible that sufficient

time was allowed for extrusion of fluid from the load-to-failure tendon before it was tested[44].

Immersion in saline causes swelling of the tendon, which increases tendon viscoelasticity; however, long-term testing with only a saline drip or atomizer does not maintain physiological hydration of the inner collagen fibrils[6,44]. The tendons tested in the marathon test were subjected to immersion in 0.10% to 0.53% saline solution. No statistical difference was found in Young's modulus values for ≥ 0.5% and < 0.5% salinity. Although it would be expected that fluid of less salinity would cause the Young's modulus value to decrease as the tendon swelled, the average Young's modulus value for tendons < 0.5% salinity was actually higher than tendons at ≥ 0.5% salinity.

A difference in Young's modulus value was found for AT tested with the load-to-failure test design (dehydrated) and with AT tested in an immersion bath of the marathon design (hydrated), so the lack of statistical difference in Young's modulus values in the varying salinities could be due to the cyclic loading. This loading pattern perhaps does not allow the tendon to swell beyond a threshold point due to the constant repetitive straightening of the collagen fibrils. Static and dynamic tests exhibit different Young's modulus values when observed on a molecular basis[43], and tensile loading has been shown to cause extrusion of water from the inside of the tendon to a bulk phase along the outside surface of the tendon[44]. For future tests however, a consistent, physiological salinity should be utilized.

Increased water content in a tendon causes increased relaxation, allowing more freedom for molecular rearrangement; whereas, a dehydrated tendon will have less freedom[22,42]. Thornton et al. found that dehydrated tendons displayed decreased creep,

as opposed to counterpart hydrated tendons, but the effects of variations in solutions were completely reversible[42]. Haut et al. also found that tendons immersed in hypotonic water relaxed faster than those immersed in hypertonic solution, meaning that more hydrated tendons would display less stiffness than less hydrated tendons[22]. This trend was found by the author in the two methods of tendon testing, with higher Young's modulus values found in the load-to-failure test method, which did not have active hydration, and lower Young's modulus values found for tendons fully hydrated in water immersion. It is assumed that the greatest influence in disparity between the two test methods on the same AT tendon resulted from hydration of the tendon. Also important to note, while Haut et al. did find differences in stiffness due to hydration, she also found that ultimate loads and elongation were not affected by the bath environment, which is important in validating the ultimate tensile test results of the CryoGrip load-to-failure test conducted by the author[22].

In addition to the effects of hydration to Young's modulus values, temperature plays an important role in viscoelastic behavior[21]. Many of the reported values in literature were derived from tests which were conducted at room temperature[10,15,36]. In the case of freeze clamps, the tendon is completely frozen within the grips and unless a source of heat is added, the mid-substance tissue of the tendon will subsequently be exposed to the cold temperatures as well, thus increasing Young's modulus values.

The CryoGrip method used in the load-to-failure test included a warm-water jacket to keep the mid-substance portion of the tendon at a physiological range of about 37° C. Freeze clamps are an accepted and popular mode of gripping because they are able to hold the tendon without slipping at high forces, and they are not destructive to the tissue

at the gripping interface[10,15,20]. The utilization of warm-water tubing is an addition to the design that helps maintain more accurate results of tendon performance in a physiological range. While the tendon exterior was maintained at about 37° C, this temperature may not have been uniformly distributed from the exterior fibers to the center of the tendon. This feature would be more of a concern for thicker tendons that have more interior tissue with further contact to the tubing envelope. The marathon test fluid was maintained at a temperature of 37° C by using a temperature probe and an internal heater; therefore, the AT tendon of this test was maintained at a steady temperature for the duration of the ~2.5 h test.

Comparison of temperature effects cannot be quantitatively calculated between the two tests because of factors such as hydration between the two test methods, but temperature is reported to have a critical effect on tendon stiffness. Wang et al determined in creep testing that there was a reduction by the order of a magnitude in tendon lifetime when temperatures were raised from room temperatures to 37°C[29]. To study potential knee laxity as a result of temperature effects on allografts during reconstructive surgery, Ciccone et al. simulated operating room conditions and exposed tensioned hamstring tendon grafts to room temperature and then increased the tendon temperature to 34°C[21]. He found that increasing tendon temperature decreased tension and stiffness by approximately 40% and 70%, respectively, thus reinstating the effects of temperature on viscoelastic properties[21]. Understanding the response of tendons to temperature and hydration through testing methods such as those administered by the author can provide critical information to surgeons and patients undergoing ACL

reconstructive surgeries. If a tendon becomes less stiff once it is exposed to warm body temperatures, laxity could be experienced by the patient.

Future Applications

The present study of EDL, FDL, FHL, and PB tendons shows promise for allocation of future allograft material. Given that most knee ligament injuries are sports-related, tendon properties under such physiological loads as running are useful to determine the most applicable tendon for a given task. In the future, allograft tendons may be selected for their mechanical properties in relation to the patient's activity of choice. A long-distance runner would select a tendon exhibiting more compliance, therefore being able to store more elastic energy, and have less hysteresis, therefore being capable of re-using more elastic energy. A football player or baseball player who has more explosive actions and requires more cutting activity would select an allograft with higher ultimate tensile strength.

A model relating the biomechanics of EDL, FDL, FHL, and PB tendons of the load-to-failure test to the biomechanics of the AT tendon in the marathon simulation would provide an extensive host of biomechanical properties in which to properly assess the efficacy of a specific allograft for implantation. An extension of the current pilot study to that end would require validation testing of the four tendons in the marathon simulation test. This would require double strands to be tested in order to sustain the frequency of the applied loads, and proper tensioning would be required to accomplish representative responses from these tendons. Given the nature of the two test methods and the different environments to which the tendons are exposed, a relationship should be established in which the factors are associated.

APPENDIX A
AVERAGE MARATHON TEST RESULTS

Table A-1. Average load and unload cycle for all marathon tendons

Duration	Extension (mm)	Force (N)	Stress (MPa)	Strain (mm/mm)
Cycle 1000	6.587	423.446	14.042	0.268
Cycle 5856	6.775	422.952	14.026	0.275
Cycle 11712	6.884	422.735	13.918	0.279

Table A-2. Average load cycle for all marathon tendons

Duration	Extension (mm)	Force (N)	Stress (MPa)	Strain (mm/mm)
Cycle 1000	6.535	416.313	13.810	0.266
Cycle 5856	6.723	413.473	13.714	0.273
Cycle 11712	6.834	412.748	13.690	0.277

Table A-3. Average unload cycle for all marathon tendons

Duration	Extension (mm)	Force (N)	Stress (MPa)	Strain (mm/mm)
Cycle 1000	6.638	430.280	14.265	0.270
Cycle 5856	6.820	432.020	14.324	0.277
Cycle 11712	6.931	432.267	14.333	0.281

APPENDIX B
MARATHON SIMULATION REGRESSION LINE EQUATIONS

Table B-1. Regression lines for rate of hysteresis

Tendon ID	Rate of Hysteresis Equations	R^2 value
1	Hysteresis Rate=-2.00E-05*ln(t)+ 0.0002	0.5746
2	Hysteresis Rate=-2.00E-05*ln(t)+ 0.0002	0.5400
3	Hysteresis Rate=-2.00E-05*ln(t)+ 0.0002	0.7556
4	Hysteresis Rate=-3.00E-05*ln(t)+ 0.0002	0.6279
5	Hysteresis Rate=-2.00E-05*ln(t)+ 0.0002	0.6144
6	Hysteresis Rate=-2.00E-05*ln(t)+ 0.0002	0.6079
7	Hysteresis Rate=-3.00E-05*ln(t)+ 0.0003	0.4474
8	Hysteresis Rate=-6.00E-05*ln(t)+ 0.0005	0.6865
9	Hysteresis Rate=-5.00E-05*ln(t)+ 0.0004	0.6433
10	Hysteresis Rate=-5.00E-05*ln(t)+ 0.0005	0.6432
11	Hysteresis Rate=-5.00E-05*ln(t)+ 0.0004	0.6292
12	Hysteresis Rate=-5.00E-05*ln(t)+ 0.0005	0.6189
13	Hysteresis Rate=-5.00E-05*ln(t)+ 0.0005	0.6233
14	Hysteresis Rate=-4.00E-05*ln(t)+ 0.0004	0.5930
15	Hysteresis Rate=-4.00E-05*ln(t)+ 0.0004	0.6101
16	Hysteresis Rate=-4.00E-05*ln(t)+ 0.0004	0.6219
17	Hysteresis Rate=-4.00E-05*ln(t)+ 0.0004	0.6793
18	Hysteresis Rate=-5.00E-05*ln(t)+ 0.0005	0.648
19	Hysteresis Rate=-5.00E-05*ln(t)+ 0.0005	0.6838
20	Hysteresis Rate=-5.00E-05*ln(t)+ 0.0005	0.6332

Table B-2. Regression lines for Young's modulus

Tendon ID	Young's Modulus Equations	R^2 value
1	E=0.7901*ln(t) +532.94	0.0212
2	E=-1.388*ln(t)+ 638.35	0.1432
3	E=-15.29*ln(t) + 631.82	0.9473
4	E=-15.06*ln(t) +461.02	0.9901
5	E=-88.00*ln(t) +1190.0	0.9342
6	E=-12.59*ln(t) +726.00	0.8845
7	E=-5.382*ln(t) +321.06	0.3764
8	E=21.116*ln(t) +398.16	0.6716
9	E=13.215*ln(t)+266.59	0.6840
10	E=13.308*ln(t) +256.49	0.6178
11	E=7.6898*ln(t)+252.88	0.7284
12	E=4.6416*ln(t)+314.45	0.1607
13	E=6.04*ln(t)+0.0181	0.3940
14	E=6.3559*ln(t)+368.71	0.3820
15	E=6.5841*ln(t)+219.27	0.6311
16	E=3.024*ln(t)+143.18	0.6997
17	E=-1.769*ln(t)+285.9	0.0402
18	E=7.5402*ln(t)+187.06	0.6357
19	E=14.626*ln(t)+255.3	0.7253
20	E=4.4479*ln(t)267.45	0.1272

Table B-3. Regression lines for strain

Tendon ID	Strain Equations	R^2
1	ε=0.0015*ln(c)+ 0.1409	0.9864
2	ε=0.001*ln(c)+ 0.1212	0.9612
3	ε=0.002*ln(c)+ 0.1139	0.9858
4	ε=0.0043*ln(c)+ 0.1612	0.9965
5	ε=0.0167*ln(c)-0.0023	0.7937
6	ε=0.0023*ln(c)+ 0.0772	0.9983
7	ε=0.013*ln(c)+ 0.3527	0.9852
8	ε=0.0025*ln(c)+ 0.2553	0.8098
9	ε=0.0023*ln(c)+ 0.2571	0.8639
10	ε=0.0029*ln(c)+ 0.371	0.8480
11	ε=0.0046*ln(c)+ 0.234	0.8116
12	ε=0.0043*ln(c)+ 0.2503	0.9264
13	ε=0.0043*ln(c)+ 0.4286	0.8631
14	ε=0.0046*ln(c)+ 0.2147	0.9459
15	ε=0.0039*ln(c)+ 0.2634	0.9253
16	ε=0.0043*ln(c)+ 0.3969	0.9213
17	ε=0.0094*ln(c)+ 0.1264	0.8471
18	ε=0.006*ln(c)+ 0.2795	0.9654
19	ε=0.0045*ln(c)+ 0.2817	0.9469
20	ε=0.0108*ln(c)+ 0.3712	0.8356

Table B-4. Regression lines for extension

Tendon ID	Extension Equation	R^2
1	Ext=0.0506*ln(c)+4.6514	0.9864
2	Ext=0.0365*ln(c)+4.2491	0.9612
3	Ext=0.0689*ln(c)+3.8596	0.9859
4	Ext=0.1491*ln(c)+5.5904	0.9965
5	Ext=0.6398*ln(c)-0.09	0.7937
6	Ext=0.0836*ln(c)+2.7473	0.9982
7	Ext=0.2512*ln(c)+6.8105	0.9852
8	Ext=0.0885*ln(c)+8.9571	0.8098
9	Ext=0.0749*ln(c)+8.2001	0.8639
10	Ext=0.0847*ln(c)+10.67	0.8480
11	Ext=0.1059*ln(c)+5.334	0.8116
12	Ext=0.1018*ln(c)+5.987	0.9264
13	Ext=0.0711*ln(c)+6.8814	0.8276
14	Ext=0.138*ln(c)+6.4162	0.9459
15	Ext=0.0822*ln(c)+5.6208	0.9253
16	Ext=0.0755*ln(c)+6.9018	0.8969
17	Ext=0.3261*ln(c)+4.3837	0.8471
18	Ext=0.1052*ln(c)+4.8413	0.9553
19	Ext=0.0892*ln(c)+5.6122	0.9469
20	Ext=0.1908*ln(c)+6.5487	0.8356

APPENDIX C
MARATHON SIMULATION: STRAIN VS. MODULUS

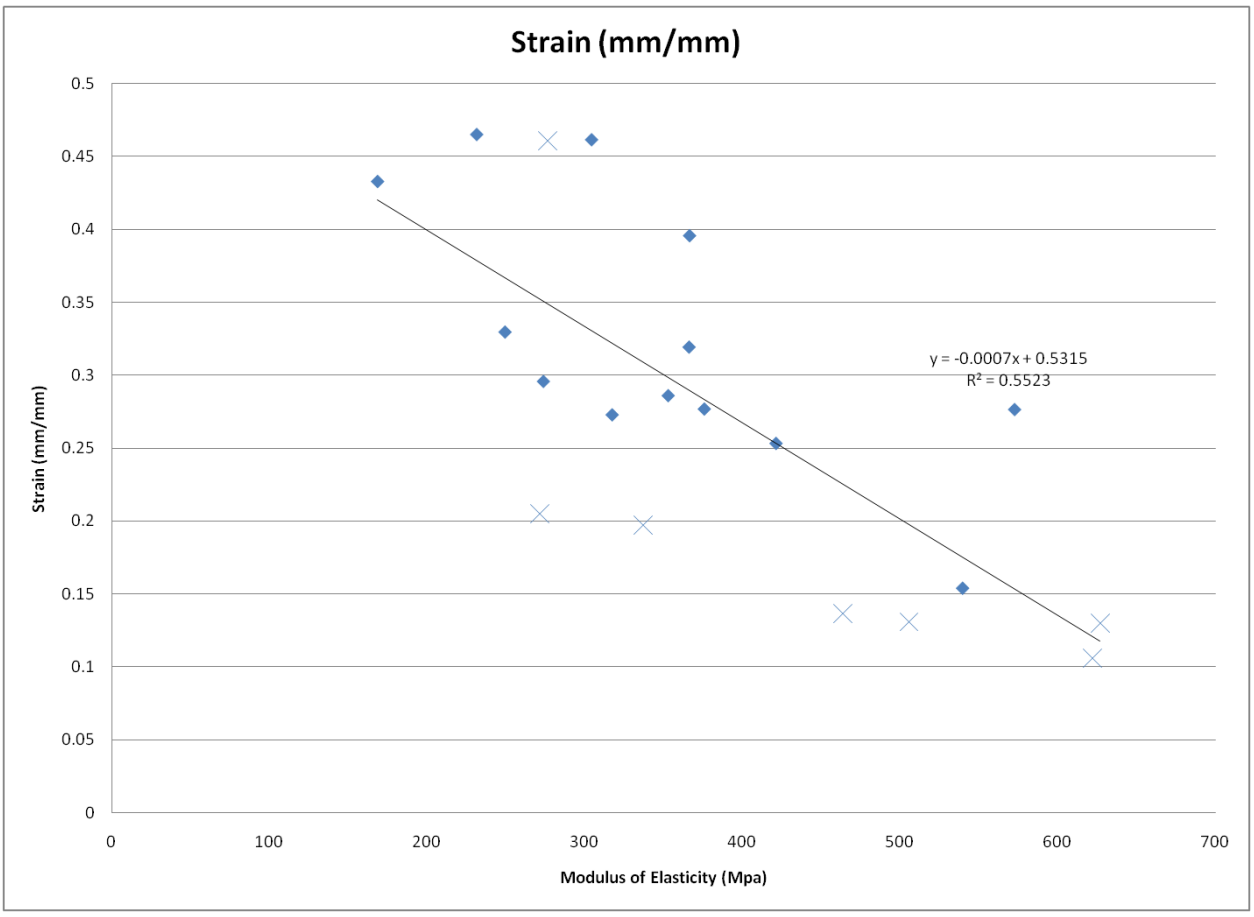

Figure C-1. Average strain vs. average Young's modulus with damaged tendons indicated by the (X) symbol. No correlation was found between strain values and Young's modulus values in relation to tendon damage.

APPENDIX D
TENTH CYCLE PERFORMANCE COMPARISON

Table D-1. Tendon comparison for each test method

Tendon	Force Profile (N)	Frequency (Hz)	Modulus Cycle 9.5 (Mpa)	Modulus Cycle 10 (Mpa)
Marathon specimen 3	50-250 N	0.67	338.56	343.66
Marathon specimen 3	250-600 N	1	528.92	534.11
CryoGrip FDL	50-250 N	1	1829.03	1863.62
CryoGrip AT	50-250 N	1	2615.62	2651.07

LIST OF REFERENCES

1. **Cohen SB, Sekiya JK**. Allograft safety in anterior cruciate ligament reconstruction. Clin Sports Med. 2007;26:597-605.

2. **Millenium Research Group**. US markets for orthopedic soft tissue solutions 2009. Toronto: Millenium Research Group, Inc, 2008.

3. **Centers for Disease Control and Prevention.** (2006, September 1). About Tissue Transplants. <http://www.cdc.gov/ncidod/dhqp/tissueTransplantsFAQ.html>.

4. **Clark JC, Rueff DE, Indelicato PA, Moser M**. Primary ACL reconstruction using allograft tissue. Clin Sports Med. 2009;28:223-44.

5. **Nagano Y, Ida H, Akai M, Fukubayashi T**. Biomechanical characteristics of the knee joint in female athletes during tasks associated with anterior cruciate ligament injury. Knee. 2009;16:153-8.

6. **Wren TA, Lindsey DP, Beaupré GS, Carter DR.** Effects of creep and cyclic loading on the mechanical properties and failure of human Achilles tendons. Ann Biomed Eng. 2003;31:710-7.

7. **Woo SL, Wu C, Dede O, Vercillo F, Noorani S**. Biomechanics and anterior cruciate ligament reconstruction. J Orthop Surg Res. 2006;1:2.

8. **Henson J, Nyland J, Chang HC, Caborn DN**. Effect of cryoprotectant incubation time on handling properties of allogeneic tendons prepared for knee ligament reconstruction. J Biomater Appl. 2008;0:1-10.

9. **Royalty RN, Junkin DM Jr, Johnson DL**. Anatomic double-bundle revision anterior cruciate ligament surgery using fresh-frozen allograft tissue. Clin Sports Med. 2009;28:311-26.

10. **Hamner DL, Brown CH Jr, Steiner ME, Hecker AT, Hayes WC.** Hamstring tendon grafts for reconstruction of the anterior cruciate ligament: biomechanical evaluation of the use of multiple strands and tensioning techniques. J Bone Joint Surg Am. 1999;81:549-57.

11. **Blythe A, Tasker T, Zioupos P**. ACL graft constructs: In-vitro fatigue testing highlights the occurrence of irrecoverable lengthening and the need for adequate (pre)conditioning to avert the recurrence of knee instability. Technol Health Care. 2006;14:335-47.

12. **Noyes FR, Barber-Westin SD**. Revision anterior cruciate surgery with use of bone-patellar tendon-bone autogenous grafts. J Bone Joint Surg Am. 2001;83:1131-1143.

13. **Steckel H, Starman JS, Baums MH, Klinger HM, Schultz W, Fu FH**. The double-bundle technique for anterior cruciate ligament reconstruction: a systematic overview. Scand J Med Sci Sports. 2007;17:99-108.

14. **Grood ES, Noyes FR**. Cruciate ligament prosthesis: strength, creep, and fatigue properties. J Bone Joint Surg Am. 1976;58:1083-8.

15. **Haut Donahue TL, Howell SM, Hull ML, Gregersen C**. A biomechanical evaluation of anterior and posterior tibialis tendons as suitable single-loop anterior cruciate ligament grafts. Arthroscopy. 2002;18:589-97.

16. **Harner CD, Xerogeanes JW, Livesay GA, Carlin GJ, Smith BA, Kusayama T, Kashiwaguchi S, Woo SL**. The human posterior cruciate ligament complex: an interdisciplinary study. Ligament morphology and biomechanical evaluation. Am J Sports Med. 1995;3:736-45.

17. **Noyes FR, Grood ES**. The strength of the anterior cruciate ligament in humans and Rhesus monkeys. J Bone Joint Surg Am. 1976;58:1074-82.

18. **Noyes FR, Butler DL, Grood ES, Zernicke RF, Hefzy MS.** Biomechanical analysis of human ligament grafts used in knee-ligament repairs and reconstructions. J Bone Joint Surg Am. 1984;66:344-52.

19. **Hollis JM, Pearsall AW, Stutz JD, Russell GV**. The biomechanical properties of the tibialis anterior, tibialis posterior, and peroneus longus tendons as potential graft sources. Poster presented at: 47th Annual Meeting, Orthopaedic Research Society; 2001 February 25-28, San Francisco, CA.

20. **Pearsall AW 4th, Hollis JM, Russell GV Jr, Scheer Z.** A biomechanical comparison of three lower extremity tendons for ligamentous reconstruction about the knee. Arthroscopy. 2003;19:1091-6.

21. **Ciccone WJ 2nd, Bratton DR, Weinstein DM, Elias JJ**. Viscoelasticity and temperature variations decrease tension and stiffness of hamstring tendon grafts following anterior cruciate ligament reconstruction. J Bone Joint Surg Am. 2006;88:1071-8.

22. **Haut TL, Haut RC**. The state of tissue hydration determines the strain-rate-sensitive stiffness of human patellar tendon. J Biomech. 1997;30:79-81.

23. **Butler DL, Guan Y, Kay MD, Cummings JF, Feder SM, Levy MS**. Location-dependent variations in the material properties of the anterior cruciate ligament. J Biomech. 1992;25:511-8.

24. **Woo SL, Abramowitch SD, Kilger R, Liang R**. Biomechanics of knee ligaments: injury, healing, and repair. J Biomech. 2006;39:1-10.

25. **Maganaris CN, Paul JP**. In vivo human tendon mechanical properties. J Physiol. 1999;1:307-13.

26. **Schimizzi A, Wedemeyer M, Odell T, Thomas W, Mahar AT, Pedowitz R.** Effects of a novel sterilization process on soft tissue mechanical properties for anterior cruciate ligament allografts. Am J Sports Med. 2007;35:612-6.

27. **Provenzano PP, Heisey D, Hayashi K, Lakes R, Vanderby R Jr**. Subfailure damage in ligament: a structural and cellular evaluation. J Appl Physiol. 2002;92:362-71.

28. **Wang XT, Ker RF, Alexander RM**. Fatigue rupture of wallaby tail tendons. J Exp Biol.1995;198:847-52.

29. **Wang XT, Ker RF**. Creep rupture of wallaby tail tendons. J Exp Biol. 1995;198:831-45.

30. **Duthon VB, Barea C, Abrassart S, Fasel JH, Fritschy D, Ménétrey J**. Anatomy of the anterior cruciate ligament. Knee Surg Sports Traumatol Arthrosc. 2006;14:204-13.

31. **Billat VL, Demarle A, Slawinski J, Paiva M, Koralsztein JP**. Physical and training characteristics of top-class marathon runners. Med Sci Sports Exerc. 2001;33:2089-97.

32. **De Zee M, Bojsen-Moller F, Voigt M**. Dynamic viscoelastic behavior of lower extremity tendons during simulated running. J Appl Physiol. 2000;89:1352-9.

33. **Boston Athletic Association**. (2009). 113th Boston Marathon Top Finishers. <http://www.bostonmarathon.org/2009/cf/public/TopFinishers.htm>.

34. **Derrick TR, Dereu D, McLean SP**. Impacts and kinematic adjustments during an exhaustive run. Med Sci Sports Exer. 2002;34:998-1002.

35. **Guyton AC, and Hall JE.** Textbook of Medical Physiology 9th edition. PA, W.B. Saunders Company. 1996; 7.

36. **Schechtman H, Bader DL**. Fatigue damage of human tendons. J Biomech. 2002;35:347-53.

37. **Pike AV, Ker RF, Alexander RM**. The development of fatigue quality in high- and low-stressed tendons of sheep (Ovis aries). J Exp Biol. 2000;203:2187-93.

38. **Fukunaga T, Kawakami Y, Kubo K, Kanehisa H.** Muscle and tendon interaction during human movements. Exerc Sport Sci Rev. 2002;30:106-10.

39. **Kubo K, Kanehisa H, Fukunaga T**. Effects of viscoelastic properties of tendon structures on stretch - shortening cycle exercise in vivo. J Sports Sci. 2005;23:851-60.

40. **Schechtman H, Bader DL.** In vitro fatigue of human tendons. J Biomech. 1997;30:829-35.

41. **Reeves ND, Narici MV, Maganaris CN**. Strength training alters the viscoelastic properties of tendons in elderly humans. Muscle Nerve. 2003;28:74-81.

42. **Thornton GM, Shrive NG, Frank CB**. Altering ligament water content affects ligament pre-stress and creep behaviour. J Orthop Res. 2001;19:845-51.

43. **Sasaki N, Odajima S**. Stress-strain curve and Young's modulus of a collagen molecule as determined by the X-ray diffraction technique. J Biomech. 1996;29:655-8.

44. **Han S, Gemmell SJ, Helmer KG, Grigg P, Wellen JW, Hoffman AH, Sotak C.** Changes in ADC caused by tensile loading of rabbit achilles tendon: evidence for water transport. J Magn Reson. 2000;144:217-27.

45. **Dubinskaya VA, Eng LS, Rebrow LB, Bykov VA**. Comparative study of the state of water in various human tissues. Bull Exp Biol Med. 2007;144:294-7.

BIOGRAPHICAL SKETCH

Meridith Myrick was born in Atlanta, Georgia where she was raised with the foundation of two loving parents and a best friend for a sister. In 2006, Meridith earned her B.S. in biological engineering with an emphasis in biomedical engineering from the University of Georgia, and remains a loyal Bulldog fan. Upon graduation, Meridith worked in the field of civil engineering in the great city of Savannah, Georgia. She quickly realized, however, that her interests were only in the biomedical field, so in 2008, Meridith enrolled in the University of Florida's J. Crayton Pruitt Family Department of Biomedical Engineering as a master's student.

Within the first month of enrollment in graduate school, Meridith received an internship position with RTI Biologics, Inc. to work with the Sports Medicine Group. She worked for them on many enriching projects, including her thesis project, which was jointly coordinated through UF and RTI Biologics, Inc.

Upon graduation from the University of Florida with a master's degree in biomedical engineering, Meridith moved back to Atlanta to start a career in the biomedical field. She will be a very joyful bride to Jon Ussery on March 27, 2010, and looks forward to a life of love, learning, and laughter.